Natural Resources Canada | Ressources naturelles Canada

GEOLOGICAL SURVEY OF CANADA
OPEN FILE 7757

Trace element signature of hydrothermal alteration assemblages (epidote, allanite, actinolite, titanite) in the footwall of the Sudbury Igneous Complex: A laser ablation ICP-MS trace element vectoring and fertility study

G. Tuba and D.E. Ames

2015

Canada

GEOLOGICAL SURVEY OF CANADA
OPEN FILE 7757

Trace element signature of hydrothermal alteration assemblages (epidote, allanite, actinolite, titanite) in the footwall of the Sudbury Igneous Complex: A laser ablation ICP-MS trace element vectoring and fertility study

G. Tuba[1] and D.E. Ames[2]

[1]Wallbrdige Mining Company Ltd., Lively, Ontario
[2]Geological Survey of Canada, Ottawa, Ontario

2015

doi:10.4095/297051

This publication is available for free download through GEOSCAN (http://geoscan.nrcan.gc.ca/)

Recommended citation

Tuba, G. and Ames, D.E., 2015. Trace element signature of hydrothermal alteration assemblages (epidote, allanite, actinolite, titanite) in the footwall of the Sudbury Igneous Complex: A laser ablation ICP-MS trace element vectoring and fertility study; Geological Survey of Canada, Open File 7757, 1 zip file. doi:10.4095/297051

Publications in this series have not been edited; they are released as submitted by the author.

Contribution to the Geological Survey of Canada's Targeted Geoscience Initiative 4 (TGI-4) Program (2010-2015)

TABLE OF CONTENTS

Figures

Tables

Trace element signature of hydrothermal alteration assemblages (epidote, allanite, actinolite, titanite) in the footwall of the Sudbury Igneous Complex: A laser ablation ICP-MS trace element vectoring and fertility study

G. Tuba[1] and D.E. Ames[2]

[1]Wallbridge Mining Company Ltd., 129 Fielding Road, Lively, Ontario P3Y 1L7
[2]Geological Survey of Canada, 601 Booth Street, Ottawa, Ontario K1A 0E8

ABSTRACT

In one of the world's largest Ni-Co mineral districts, geophysical methods have been successfully employed for detecting the traditional Sudbury contact and offset types of Ni-Cu-PGE ore for over a century. Discoveries of low-sulphide, high-PGE tenor orebodies, defined in 2005 (i.e. McCreedy West PM zone), in the footwall environment to the Sudbury Igneous Complex (SIC), caused explorationists to focus on the detection of these precious metal-rich resources that are hosted in randomly distributed impact-derived breccia entirely within Archean and Proterozoic country rocks. These zones of Sudbury breccia host two styles of footwall-type deposits: a) high-sulphide vein-style Cu-PGE ores (i.e. Strathcona, McCreedy East 153 chalcopyrite veins), widely recognized with a magmatic-hydrothermal origin and b) low-sulphide disseminations, blebs, and stringers with high platinum group element (PGE) tenor and dominated by silicate assemblages of hydrothermal origin. Due to the absence of chalcopyrite or sulphide minerals, this second footwall ore-style is a challenge to detect in the field using the geophysical methods traditionally used for magmatic deposits and thus, identifying key hydrothermal alteration assemblages and developing discriminant mineral chemistry diagrams could yield criteria for these hydrothermal footwall ores.

Proper classification is important for guiding future exploration for the low-sulphide metal-rich deposits in the footwall to the Sudbury Igneous Complex. The aim of the study was to establish typical element-associations and behaviours for the paragenetically different hydrothermal assemblages produced during the diverse post-impact magmatic-hydrothermal history of the footwall and hanging-wall units along the North and East ranges of the Sudbury structure to potentially detect a unique signature for alteration related to the high-tenor PGE mineralization.

This TGI4 Ni-PGE Project data release contains geochemical databases of (a) laser ablation ICP-MS mineral chemistry of epidote, allanite, amphibole, and titanite, from 62 samples and (b) whole-rock geochemistry of least-altered host-rock types. Epidote and amphibole in the alteration assemblages exhibit host-rock-normalized REE plots with characteristic topologies that are best described with nLREE to nHREE relations, and though groups of alteration types are REE-enriched, other groups are REE-poor including the PGE- mineralized alteration assemblage. Thus REE contents and patterns are not discriminants for detection of low-sulphide, high-PGE mineralization.

Trace element partitioning occurs between texturally coeval minerals, such as epidote and amphibole (REE, Pb, Bi, Sn: shows affinity to epidote; Co, Ni, Zn: shows affinity to amphibole), as well as titanite and amphibole (REE, Sn, Zr, Nb, Yb, Th, U: affinity to titanite; Co, Ni, Zn: affinity to amphibole). This scavenging phenomenon greatly affects the element distribution of the mineral pairs; therefore, conclusions drawn on the trace element concentrations of a single mineral should be avoided. The trace element concentration of epidote/amphibole may be influenced by (1) the parental fluid composition (e.g. REE, U, Th, Ni, Pb, Sn), (2) the host rock, particularly mafic rocks (e.g. As, Zn) and/or (3) the crystal structural properties of the minerals (e.g. Mg and Sr in epidote).

The pathfinder elements Ni, Pb, Sn, and Co in epidote and amphibole are the most reliable elements to fingerprint distinctly the PGE mineralizing alteration in the footwall. Both epidote and amphibole of mineralized sulphide-silicate and generally barren extensional assemblages show systematic differences in the concentrations of key pathfinders among different locations along the North and East ranges.

INTRODUCTION AND BACKGROUND

In situ trace element analyses were carried out on silicate minerals from a number of representative alteration assemblages of several hydrothermal events and/or stages that followed the Sudbury impact at 1850 Ma. The aim of the study was to establish typical element associations and behaviours for the paragenetically different hydrothermal assemblages, especially those that characterize the mineralizing fluids associated with the low-sulphide, high-precious metal miner-

alization (LSHPM) in the footwall to the Sudbury Igneous Complex. In the absence of chalcopyrite or other sulphide minerals, the LSHPM mineralization is a challenge to detect in the field using geophysical methods. Thus proper identification and classification of key hydrothermal alteration assemblages and developing discriminant mineral chemistry diagrams may lead to a vectoring tool for exploration.

This study was funded as part of the Targeted Geoscience Initiative (TGI-4) Ni-Cu-PGE project (Ames and Houlé, 2011; Ames et al., 2012), building on the Ph.D. studies of the first author on the Wisner South, Southwest, and Amy Lake Cu-PGE occurrences (Tuba, 2012; Tuba et al., 2010, 2014). Sample suites from previous studies (Ames, 1999; Ames and Farrow, 2007; Ames et al., 2008; Tuba, 2012), which included a comprehensive alteration sample suite of the lower economic ore zones and upper parts of the Sudbury structure hydrothermal system (Ames and Farrow, 2007; Ames et al., 2008), was expanded to cover more areas and alteration types. Samples from the economic ore zones in the Levack embayment were included along with a broad distribution of samples from sub-economic exploration showings across the North Range, as well as samples of non-mineralized regional alteration types (Table 1). This provided for a more complete representation of the Sudbury hydrothermal system allowing the characterization of additional trace minerals and alteration and mineralization styles.

This data release contains geochemical databases of (a) laser ablation ICP-MS mineral chemistry of epidote, allanite, amphibole, and titanite, and (b) whole-rock geochemistry of least-altered host-rock types. Silicate minerals of 39 samples were analyzed for trace element compositions as part of the TGI-4 Ni-PGE Project (Ames and Houlé, 2015). The sample suite was supplemented by full or partial analyses of 25 samples that had been previously published (Tuba, 2012; Tuba et al., 2014); thus, the database contains epidote, allanite, amphibole, and titanite (where applicable) trace element concentrations from a total of 62 samples representing 8 alteration types that were described from the Sudbury footwall and hanging-wall units (Tables 1 and 2).

GEOLOGICAL SETTING AND THE SUDBURY HYDROTHERMAL SYSTEM

The Sudbury structure is the product of a comet impact (Pope et al., 2004, Petrus et al., 2014) that took place 1850 Ma ago (Krogh et al., 1984) resulting in a prominent and economically significant feature, the Sudbury Igneous Complex (SIC), which hosts the Ni-Cu-PGE ores in the Sudbury mining camp. The originally flat-lying, ~150–200 km x 3 km SIC was tectonically deformed, folded into a doubly plunging syncline and eroded into its present shape. The large impact-generated hydrothermal system (Ames et al., 1998), fuelled from the heat of the cooling SIC and impact event, circulated fluids through the breccia units above and below the SIC (Farrow and Watkinson, 1992; Li and Naldrett, 1994; Hanley and Mungall, 2003; Hanley et al., 2004; Ames et al., 2006).

Hydrothermal fluids above the SIC generated regional semi-conformable silicification, albite-actinolite and carbonate alteration of the andesitic Onaping Formation (1848 Ma: Ames et al., 1998), and VMS-like hydrothermal Zn-Pb-Cu deposits on the paleoseafloor 1.5 km above the SIC. The Archean and Paleoproterozoic footwall to the SIC has multiple alteration styles, types and generations of pre-, syn-, and post-impact hydrothermal events. For a more thorough discussion, the reader is referred to the extensive literature about the Sudbury mine environment, which describes the sources, physical and chemical conditions, and exploration of the SIC (Farrow and Watkinson, 1992; Jago et al., 1994; Li and Naldrett, 1994; Molnár et al., 2001; Hanley et al., 2004; Hanley and Bray, 2009 and references there-in).

Groundwater, deep crustal fluids, seawater (if present), and basement fluids commonly recharge an impact site after initial volatilization of both impacted materials and the bolide, and the crust is melted, faulted, and cooled. Circulation of mixed fluids and volatiles is dependent on host-rock permeability and may utilize permeable pathways, such as impact-derived breccia units developed around the transient crater in the target rocks (pseudotachylite/cataclasite; e.g. Sudbury Breccia) as well as deep-seated and shallow fault structures of the final modified crater (Melosh, 1989; Abramov and Kring, 2004). Evidence for fluids in the impact structure, including the regional distribution of hydrothermal alteration mineralogy as evidence for fluid and volatile flow, below, within and above the SIC, the fluid/volatile sources, origin and its role, has been presented by Farrow and Watkinson (1992), Ames et al. (1998), Farrow and Watkinson (1999), Hanley et al. (2005, 2011), Ames and Farrow (2007), Campos-Alvarez et al. (2010), Tuba et al. (2014), Kerr et al. (2015) and others.

METHODOLOGY

Sample suite (collection)

A suite of 62 samples, representing 8 alteration types in the footwall and hanging wall of the Sudbury Igneous Complex (SIC), were studied (Fig. 1). Samples collected from the North Range footwall include the Morrison deposit – Deep zone, McCreedy West deposit – PM zone, Podolsky deposit – North zone, Broken Hammer deposit – epidote-sperrylite zone, which all have economic low-sulphide mineralization. Sub-eco-

Table 1. Summary of samples and minerals analyzed in the trace element study.

		Minerals analyzed			
Sample	**Location**	Epidote	Allanite (and REE-epidote)	Amphibole	Titanite
06AV-30B	Broken Hammer	FW min/poikilitic			
06AV-37A	Broken Hammer	FW min/euhedral			
06AV-38	Broken Hammer	FW min/poikilitic			
06AV-47F	Broken Hammer	extensional			
12AV-15B	Broken Hammer Sperrylite zone	FW min/poikilitic		extensional	
12AV-16A	Broken Hammer Sperrylite zone	extensional			
12AV-17	Broken Hammer Sperrylite zone	extensional			
12AV-18X	Broken Hammer Sperrylite zone	euhedral			
AV-488B	Capreol			extensional	
12AV-53	Frost Amy Lake	*extensional*			
12AV-58	Frost Amy Lake	*pre-S perv/euhedral*			
12AV-59	Frost Amy Lake	*pre-S perv/euhedral*			
12AV-60	Frost Amy Lake	pre-S perv/euhedral	*pre-S perv/core, REE-epidote rims*	pre-S perv/euhedral, pre-S perv/halo	
12AV-61	Frost Amy Lake	pre-S perv/euhedral			
12AV-62	Frost Amy Lake	*pre-S vein/euhedral*			
12AV-63	Frost Amy Lake	pre-S vein/euhedral		pre-S vein/halo	pre-S vein/euhedral
12AV-64	Frost Amy Lake	pre-S vein/euhedral		pre-S vein/halo	
12AV-65	Frost Amy Lake	pre-S vein/euhedral		pre-S vein/halo	
12AV-69	Frost Amy Lake	FW min/poikilitic		FW min/euhedral	
12AV-70	Frost Amy Lake	*FW min/poikilitic*		*FW min/euhedral*	
12AV-77	Frost Amy Lake	*post-Sudbury/shear-type*			
12AV-78	Frost Amy Lake			extensional	extensional
12AV-80	Frost Amy Lake	FW min/poikilitic		FW min/euhedral	
FAL-12	Frost Amy Lake	*FW min/poikilitic*		*FW min/euhedral*	
FST-03	Frost Amy Lake	*post-Sudbury/shear-type*			
L400-04	Frost Amy Lake	pre-S perv/pervasive			FWGR/miarolitic
L400-07	Frost Amy Lake			extensional	
WC-013 173.6	Frost Amy Lake	*FW min/poikilitic*		*FW min/euhedral*	
AV-514B	Joe Lake			amygdule	
AV-524A	Joe Lake			amygdule	
AV-532B	Joe Lake				alteration halo
AV-J3	Joe Lake			amygdule	
08AV-04C	Lower Morrison deposit	*FW min/poikilitic*			
08AV-05A	Lower Morrison deposit	*FW min/poikilitic, pre-S perv/euhedral*	pre-S perv/core, REE-epidote rims	FW min/euhedral	
05AV-24A	McCreedy W PM zone	FW min/poikilitic		FW min/euhedral	
05AV-25B	McCreedy W PM zone	*FW min/poikilitic*			
05AV-26A	McCreedy W PM zone	*FW min/poikilitic*			
05AV-28A	McCreedy W PM zone	*FW min/poikilitic*			
02AV-642	Podolsky	FW min/poikilitic		FW min/euhedral	
11AV-57C	Podolsky	pre-S perv/euhedral		FW min/euhedral	
11AV-57D	Podolsky		pre-S perv/core, REE-epidote rims		
11AV-62F	Podolsky	FW min/poikilitic		FW min/euhedral	

Table 1 continued.

Sample	Location	Minerals analyzed			
		Epidote	Allanite (and REE-epidote)	Amphibole	Titanite
604051	Trill		amygdule	amygdule	amygdule
12AV-55	Trill	*extensional*			
TR-1005	Trill		amygdule	amygdule	amygdule
20070227	Windy Lake	*FWGR/miarolitic*			
12AV-57	Windy Lake	FWGR/miarolitic			FWGR/miarolitic
12AV-76	Wisner South	*post-Sudbury/shear-type*			
SZE-08	Wisner South	*post-Sudbury/shear-type*			
12AV-50	Wisner Southwest	*extensional*			
12AV-51	Wisner Southwest	*extensional*			
12AV-66	Wisner Southwest	*FW min/poikilitic*			
12AV-68	Wisner Southwest	*FW min/poikilitic*		*FW min/euhedral*	
12AV-73	Wisner Southwest	*post-Sudbury/shear-type*			
BLT-03	Wisner Southwest			extensional	extensional
BLT-05	Wisner Southwest			extensional	
BLT-06	Wisner Southwest	in extensional amphibole vein		extensional	
RRT-07	Wisner Southwest	*post-Sudbury/shear-type*			
WIS-014 766.83	Wisner Southwest	*extensional*			
06AV-52A	Wisner West	FW min/poikilitic			
06AV-55B	Wisner West	extensional			
06AV-56A	Wisner West	FW min/poikilitic			

Samples and mineral analyses in italic are from Tuba (2012) and Tuba et al. (2014).

Abbreviations: FWGR = footwall granophyre, FW min = footwall mineralization sulphide-silicate assemblage, pre-S perv = pre-sulphide pervasive assemblage, pre-S vein = pre-sulphide vein assemblage.

Table 2. Morphology and textures of analyzed minerals in the studied alteration assemblages.

Alteration type	Epidote	Allanite	Amphibole	Titanite	Mineralization style
Miarolitic cavities (3)	coarse prismatic	in epidote core	coarse euhedral	euhedral	barren
Pre-sulphide pervasive epidote-amphibole alteration (8)	coarse prismatic	in epidote core	coarse euhedral; fibrous in halo		occasionally high PGE; barren
Pre-sulphide epidote vein (4)	coarse prismatic		fibrous in halo	euhedral	barren
Broken Hammer epidote-sperrylite assemblage (1)	coarse prismatic				high PGE
Footwall mineralization, extensional epidote-quartz (9) and amphibole vein (7)	coarse prismatic (in epidote-quartz veins)		acicular euhedral (in amphibole veins)	euhedral (in amphibole veins)	occasionally high PGE; barren
Footwall mineralization, sulphide-silicate assemblage (22)	poikilitic		euhedral		high- and low-sulphide, high PGE
Amphibole amygdules (5)		euhedral (Trill only)	acicular (Trill) coarse euhedral (Onaping)	coarse euhedral (Trill only)	barren
Post-Sudbury shear-type veins (6)	fine- to medium-grained euhedral				barren

Number of samples analyzed in each alteration group indicated in brackets. Note that some samples contain more than one alteration assemblages.

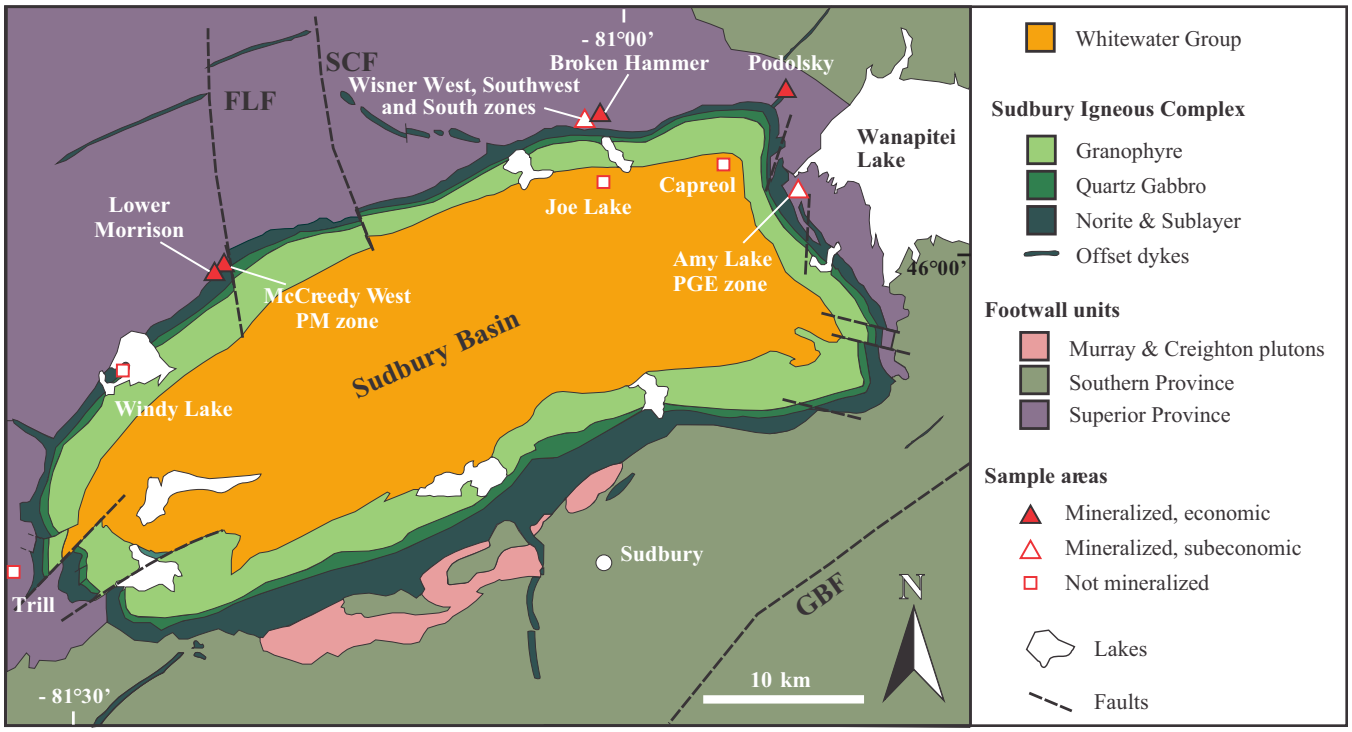

Figure 1. General geology of the Sudbury structure with sample and deposit locations used in this study. (After Ames et al., 2005.)

nomic low-sulphide mineralization was sampled from exploration trenches at Wisner West, Southwest, and South zones (North Range) as well as from the Amy Lake Cu-PGE zone (East Range) (Fig. 1). Samples were also collected from the hydrothermally altered SIC footwall at Trill and Windy Lake (Tuba, 2012), as well as from the Joe and Rockcut Lakes hanging-wall environment (Ames and Gibson, 2004a,b), which, though barren, have similar mineral assemblages to some of the alteration types found in mineralized areas.

Whole-rock geochemistry

Whole-rock geochemistry was done by commercial and federal government labs (pre-2005), including ALS Chemex and Activation Laboratories as noted in the database (Table A1). Whole-rock geochemical compositions, provided by Wallbridge Mining Company Limited (Lively, Ontario), were determined by ALS Chemex using the ME-MS61 ultra-trace method, which includes both ICP-AES and ICP-MS analyses; Pt, Pd, Au, and Ag concentrations were determined by using the PGM-ICP23 procedure. Compositions of samples analyzed by Actlabs were determined via fusion digestion followed by ICP-OES for whole-rock data and rare earth elements, ICP-ISE for fluorine, and ICP-MS for trace elements; INAA was also used to analyze chlorine and nickel. Fire assay followed by ICP-MS was used for gold, palladium, and platinum; infrared absorption was used for carbon and sulfur; and total iron in concentrate by titration.

Chemical analyses of some samples were conducted at the Geological Survey of Canada, Ottawa. Major element analyses were determined by wavelength dispersive XRF, and FeO, H_2O total, CO_2, C, and S were determined by infrared absorption (LECO). Trace elements were determined using inductively coupled plasma emission (ICP-ES) and mass spectroscopy (ICP-MS). Zirconium was determined by XRF, except at concentrations below 100 ppm where ICP-MS was used. Fluorine, Cl, and S were determined using a method based on pyrohydrolysis and anion-ion chromatography. Precision and accuracy was better than 5%: 2 sigma RSD with measurements made relative to in-house reference material, duplicate samples, and international standards.

The mineral chemical analyses were normalized to the bulk host-rock composition of each sample to eliminate the effects of fluid-rock interaction, which were significant in some of the alteration assemblages (Tuba et al., 2014). The least-altered compositions of host rocks used in the study are summarized in Table A1.

Electron microprobe analysis

Mineral chemical data were obtained using a Camebax MBX electron microprobe at Carleton University, Ottawa. Operating conditions for silicate measurements were 15 kV and 15 nA. A counting time of 40 s and 60 s was applied for F and Ni, respectively. All other elements were analyzed using counting times of 15–20 s or a maximum of 40,000 counts. Electron

microprobe analysis of epidote was also carried out at the University of Leoben, Austria, using a JEOL JXA 8200 microprobe, and with a Cameca SX-50 at the Geological Survey of Canada. Wavelength-dispersive X-ray spectroscopy was conducted using operating conditions of 15 kV and 20 nA.

Laser ablation ICP-MS analysis

Laser ablation ICP-MS trace element analyses of epidote, allanite, amphibole, and titanite were completed at the Geological Survey of Canada, Ottawa (Table 3). An Analyte.193 laser ablation sampler (Photon Machines Inc.), based on an ArF excimer laser ($\lambda = 193$ nm), was coupled to an Agilent 7700x quadrupole ICP-MS running in standard configuration with an addition of a second interface rotary pump, which approximately doubles instrument sensitivity. Data were acquired on selected isotopes of 54 elements for 100 s, starting with a 40-second period where only the gas blank was collected. An average of 10 grains were ablated on each sample, using spot analysis and bracketed between runs of the calibration standards analyzed twice, at the beginning and end of the analytical session. Laser spot diameter was typically 34–52 μm for epidote and 26–34 μm for the other minerals analyzed, at a wavelength of 193 nm and a repetition rate of 10 Hz. The CaO content of the samples, determined beforehand by means of electron microprobe analysis, was used as an internal standard for the GSD-1G calibration standard. The FeO value gained by laser ablation served as the internal standard for Po726 that was used for calculating the concentration of Pt, Pd, and Rh in the samples. All values were compared to reference material BCR-2G. For quality control purposes, measured values for USGS basaltic glass reference material BCR-2G (http://crustal.usgs.gov/geochemical_reference_standards/microanalytical_RM.html) were compared against compiled literature values (GeoReM Preferred values; http://georem.mpch-mainz.gwdg.de). Detection limits were calculated for each individual analysis to take into account differing ablation yields.

Table 3. Laser ablation ICP-MS operating conditions.

LA	
Wavelength	193 nm
Repetition rate	10 Hz
Pulse duration (FWHM)	4–6 ns
Spot diameter	26–52 μm
Energy density	6.42 J/cm^2
Calibration standards	GSD-1G, Po726
Reference material	BCR-2G
ICP-MS	
Model	Agilent 7700x
Forward power	1200 kW
Shield torch	Used
Sampling depth	6.2 mm
Gas flows:	
Carrier (He)	1 L/min
Make up (Ar)	1.02 L/m
ThO^+/Th^+	≤0.2%
Data acquisition parameters	
Data acquisition protocol	Time Resolved Analysis
Scanning mode	Peak hopping, 1 point per peak
Isotopes determined	^{25}Mg, ^{27}Al, ^{29}Si, ^{34}S, ^{422}Ca, ^{45}Sc, ^{49}Ti, ^{51}V, ^{53}Cr, ^{55}Mn, ^{57}Fe, ^{59}Co, ^{60}Ni, ^{65}Cu, ^{66}Zn, ^{75}As, ^{85}Rb, ^{88}Sr, ^{89}Y, ^{90}Zr, ^{93}Nb, ^{95}Mo, ^{103}Rh, ^{105}Pd, ^{107}Ag, ^{108}Pd, ^{111}Cd, ^{118}Sn, ^{121}Sb, ^{133}Cs,^{137}Ba, ^{139}La, ^{140}Ce, ^{141}Pr, ^{146}Nd, ^{147}Sm, ^{151}Eu, ^{157}Gd, ^{159}Tb, ^{163}Dy, ^{165}Ho, ^{167}Er, ^{169}Tm, ^{173}Yb, ^{175}Lu, ^{195}Pt, ^{197}Au, ^{201}Hg, ^{206}Pb, ^{207}Pb, ^{208}Pb, ^{209}Bi, ^{232}Th, ^{238}U
Dwell time per isotope	10 ms, except: 5 ms: ^{25}Mg, ^{27}Al, ^{29}Si, ^{49}Ti, ^{51}V, ^{55}Mn, ^{88}Sr, 15 ms: ^{103}Rh, ^{108}Pd, ^{109}Ag, ^{133}Cs, ^{195}Pt, ^{197}Au, ^{208}Bi
Quadrupole settling time	1–5 ms depending upon mass jump
Analysis time	100 seconds

GEOLOGY OF THE STUDIED AREAS

Areas with economic footwall mineralization

The Levack-Strathcona embayment contains 19 Ni-Cu-PGE contact and footwall-style deposits and is by far the most lucrative region along the North Range (Ames and Farrow, 2007). Two deposits recognized and discovered in the last decade, the McCreedy West and Morrison deposits, host LSHPM mineralization in a zone of Sudbury Breccia that formed as a product of meteorite impact into Archean gneiss. The McCreedy West deposit precious metal (PM) zone is the type area for LSHPM where the economic significance of this new ore style was realized (Farrow et al., 2005). Low-sulphide yet high-precious metal contents were also intersected below the present mine workings in drill core at 550 to 600 m true depth below the SIC, deep within the Morrison deposit (Ames and Kjarsgaard, 2013).

The Wisner property is located in the stratigraphic footwall of the Wisner embayment (Fig. 1), which hosts several small contact-type Ni-Cu-PGE deposits (WD-16, WD-13). The area contains abundant impact brecciated units of felsic to intermediate gneiss, migmatite, and mafic bodies of the Archean Levack Gneiss Complex, as well as quartz monzonite of the Cartier Batholith. Diabase dykes of the Matachewan swarm and units of Wisner Gabbro related to the 2657±9 Ma Joe Lake intrusion (Bleeker et al., 2013, 2015) represent volumetrically the most significant mafic intrusive rocks in the area.

The Broken Hammer Open Pit is situated 1.3 km laterally from the present SIC contact (estimated ~600 m true depth) exposing mineralization hosted by brecciated quartz monzonite and minor mafic units (Matachewan diabase, Wisner Gabbro). Sudbury Breccia hosts up to 1 m wide massive sulphide veins

accompanied by low-sulphide assemblages (Péntek et al., 2008). In the footwall of one of the major sharp-walled veins, the Broken Hammer sperrylite zone, a few metres wide, silicate-hosted high-PGE zone was discovered in 2011 (Wilson, 2012; Ames et al., 2013, 2014).

At the past-producing Whistle Open Pit mine, the Whistle radial offset structure hosts Ni-Cu contact ore in the embayment at the intersection of the SIC main mass and a northeast-trending offset structure (Lightfoot et al., 1997). Situated ~650 m below the contact ore and along the Whistle Offset structure, the Podolsky Cu-Ni-PGE deposit was discovered by FNX in the reclamation stage of Vale's Whistle Open Pit. It was in production from 2005 to 2012, yielding ~1.5 Mt of 4.29% Cu, 0.38% Ni, 0.051 oz/t Pt, 0.054 oz/t Pd, and 0.024 oz/t Au between 2007 to 2011 (MacInnis et al., 2014) Podolsky is a hybrid deposit that displays both sharp-walled and low-sulphide elements of footwall mineralization systems in the 2000 deposit zone (Farrow et al., 2005). Cu-PGE veins and stockwork occur within and adjacent to a large Archean gabbroic block within breccia in the Offset structure (Farrow et al., 2005; Ames and Farrow, 2007; Carter et al., 2009; MacInnis et al., 2014).

Areas with subeconomic footwall-style mineralization

Wisner West, Southwest, and South zones, North Range

The mineralized Wisner West (Vale), Southwest and South zones (Wallbridge) are a series of showings within a breccia zone subparallel to, and at a 500 m lateral distance from, the present-day SIC contact and 1.5 to 3.5 km west-southwest of the Broken Hammer Open Pit (Fig. 1). Subeconomic low-sulphide mineralization in these areas is typified by sulphide patches and veins associated with Sudbury Breccia. The breccia is thermally metamorphosed and cut by abundant veins and pockets of footwall granophyre (Tuba et al., 2010; Péntek et al., 2011).

Amy Lake platinum group element zone, East Range

The Amy Lake PGE zone (Fig. 1) is hosted within a northwest-trending, ~2.5 km long by 100 m wide Sudbury Breccia belt that also hosts the subsurface Capre 3000 footwall deposit 800 m to the south. It occurs at a 600 m lateral distance from the SIC contact, within brecciated mafic-intermediate Levack Gneiss, Cartier Granite, Matachewan diabase and gabbro (Tuba et al., 2014). Thermal metamorphism and partial melting in the Amy Lake zone is manifested by numerous footwall granophyre dykes and in situ melt pockets cutting the footwall units and Sudbury Breccia. Low-sulphide mineralization (patches and short veinlets) is present in areas dominated by mafic host rocks, and is structurally controlled by the northwest-trending Bay Fault zone.

Non-mineralized areas below and above the Sudbury Igneous Complex

Alteration below the Sudbury Igneous Complex

Two areas with extensive hydrothermal alteration, yet no sulphides, were studied in the Trill and Windy Lake footwall environments. At Trill, hydrothermally altered, massive Sudbury Breccia is exposed on two outcrops with a total surface area over 34,000 m^2, about 3 km west from the SIC contact (Fig. 1). The breccia has an aphanitic, glassy matrix hosting monzonite (of the Cartier Batholith) and Matachewan diabase clasts of variable sizes, ranging from a few millimetres to 5 metres in diameter (Tuba, 2012).

At Windy Lake, impact brecciated units of Levack Gneiss dominate the footwall to an embayment that hosts subeconomic disseminated Ni-Cu-PGE mineralization. Footwall mineralization is not known in the area.

Alteration above the Sudbury Igneous Complex in the Onaping Formation

Two areas with intense alteration in the lower breccia units of the Onaping Formation were studied at Joe Lake and Rockcut Lake, along the North Range of the Sudbury structure (Ames and Gibson, 2004a,b). The andesite breccia is intruded along northwest-trending growth faults in the lower Sandcherry member by aphanitic dykes and is generally albitized and lacks sulphide.

ALTERATION ASSEMBLAGES

Hydrothermal alteration, dominated by epidote and/or amphibole, occurs as miarolitic cavities, pervasive replacement, veins and disseminations in pre-, syn-, and post-impact paragenetic sequences. Proper classification and chemical fingerprinting is important for guiding future exploration.

A comprehensive synopsis of the studied alteration assemblages is presented here; however, for more detailed descriptions refer to Ames et al. (1998, 2006), Ames (1999), Péntek (2009), Tuba et al. (2010, 2014), Péntek et al. (2011), and Tuba (2012). More extensive field photos and photomicrographs of the alteration types can be found in the Ph.D. theses of the authors (Ames, 1999; Tuba, 2012). Figure 2 presents the paragenetic order of the assemblages in the footwall environment.

"Pre-sulphide" assemblages related to footwall granophyre

Three types of alteration assemblages that predate the main footwall sulphide mineralization include (1) epi-

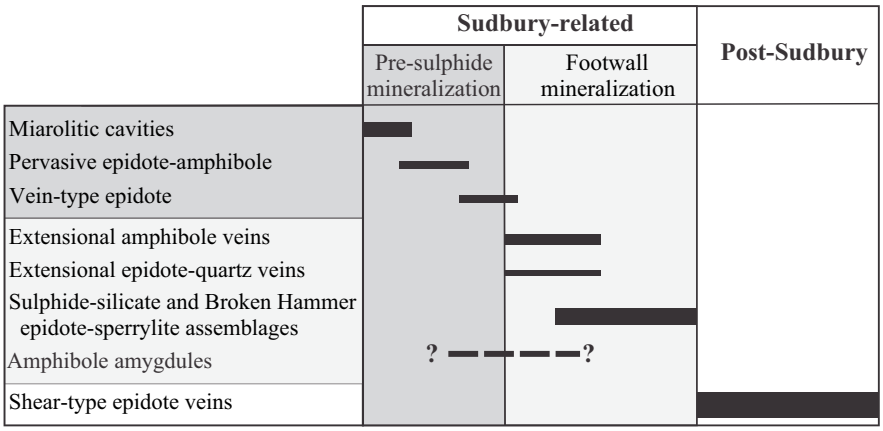

Figure 2. Paragenetic order of the studied mineral assemblages (after Tuba, 2012 and Tuba et al., 2014). Amphibole amygdules are early and likely contemporaneous to the mineralized footwall systems, but exact temporal relationship to other assemblages could not be established due to lack of textural evidence.

dote-amphibole-allanite-titanite within miarolitic cavities in footwall granophyre veins and pods, (2) pervasive epidote-amphibole patches, and (3) epidote veins (Fig. 3). This alteration group is interpreted to have formed from high-temperature (>400°C), high-salinity (>30 NaCl equiv. wt%) magmatic-hydrothermal fluids that are spatially linked to the footwall granophyre (FWGR) bodies in the Sudbury footwall, and predates the main sulphide ore-forming event that resulted in the formation of footwall deposits (Péntek et al., 2013; Tuba et al., 2014).

Miarolitic cavities, measuring up to tens of centimetres in diameter, are very common features within the FWGR bodies (Fig. 3a) and are the product of in situ crystallization of a segregated magmatic fluid from the silicate melt (e.g. Molnár et al., 2001; Péntek et al., 2011). Miarolites are typically filled by quartz, albite, and K-feldspar, as well as epidote, Ni-rich amphibole, minor allanite and titanite, and trace zircon and apatite (Péntek, 2009). The studied miarolitic Windy Lake samples are dominated by epidote, quartz, and minor titanite.

Pervasive epidote-amphibole assemblages may form a halo to FWGR veins, but frequently occur physically detached from them, as up to a couple of metres wide alteration zones in the country rock (Tuba et al., 2014) (Fig. 3b to d). The assemblage is dominated by coarse prismatic epidote with about 35% actinolite and quartz, the ratio of which is dependent on the host-rock composition. Minor allanite may appear in the cores of the coarse epidote grains (Fig. 3e). Pervasive epidote-amphibole zones bearing disseminated millerite (<15%) and abundant platinum group minerals (PGM; dominantly sperrylite and merenskyite/moncheite) are known from the Amy Lake PGE zone (Tuba et al., 2014).

Epidote veins (Tuba et al., 2014) that are found in isolation from FWGR bodies (Fig. 3f) are 1 to 2 cm wide and consist dominantly of coarse epidote with minor to trace titanite, trace quartz, and rare allanite. Sulphide minerals were not observed. Both pervasive epidote-amphibole patches and vein-type pre-sulphide assemblages are surrounded by a characteristic composite halo comprising a proximal actinolitic and a distal recrystallized feldspar zone in mafic rocks (Fig. 3f).

Hydrothermal assemblages contemporaneous with the Sudbury Igneous Complex footwall mineralization

Low-sulphide mineralization may have formed by the mobilization of base and precious metals from a pre-existing magmatic source and the transport of these metals along brittle structures by hydrothermal fluids (e.g. Farrow et al., 2005; Nelles et al., 2010; Tuba et al., 2010, 2014; Hanley et al., 2011; Péntek et al., 2013). Hydrothermal alteration in these low-sulphide zones also produced sulphide-free extensional veins that represent a different stage of the same high-temperature, high-salinity hydrothermal system (Tuba et al., 2010, 2014). Extensional epidote-quartz and amphibole veins without accompanying mineralization were found in the footwall in areas lacking a metal source (Tuba et al., 2010; Tuba, 2012); they also occur in the hanging wall of the Sudbury Igneous Complex (Ames et al., 1998; Ames and Gibson, 1995).

Both massive sharp-walled chalcopyrite veins and low-sulphide samples (few-cm chalcopyrite veins, patches, and disseminations) have a uniform texture with the central sulphide mass being surrounded by an extensive hydrous silicate selvage (Fig. 4a to c). The characteristic feature of this sulphide-silicate assemblage is poikilitic epidote that dominates the silicate selvage and contains numerous inclusions of chalcopyrite, PGM, and other trace minerals (Farrow, 1994; Kjarsgaard and Ames, 2010; Tuba et al., 2010, 2014; White, 2010) (Fig. 4d). It may be accompanied by minor to trace amounts of euhedral, Ni-bearing amphibole (Fig. 4e,f) and trace amounts of quartz and Ni-bearing chlorite, the latter of which was not observed in the studied samples. For a detailed description of the sulphide and PGM mineral composition of Sudbury footwall systems, refer to Farrow (1994), Farrow and Watkinson (1999), Farrow and Lightfoot (2002), and Ames and Farrow (2007) and references therein.

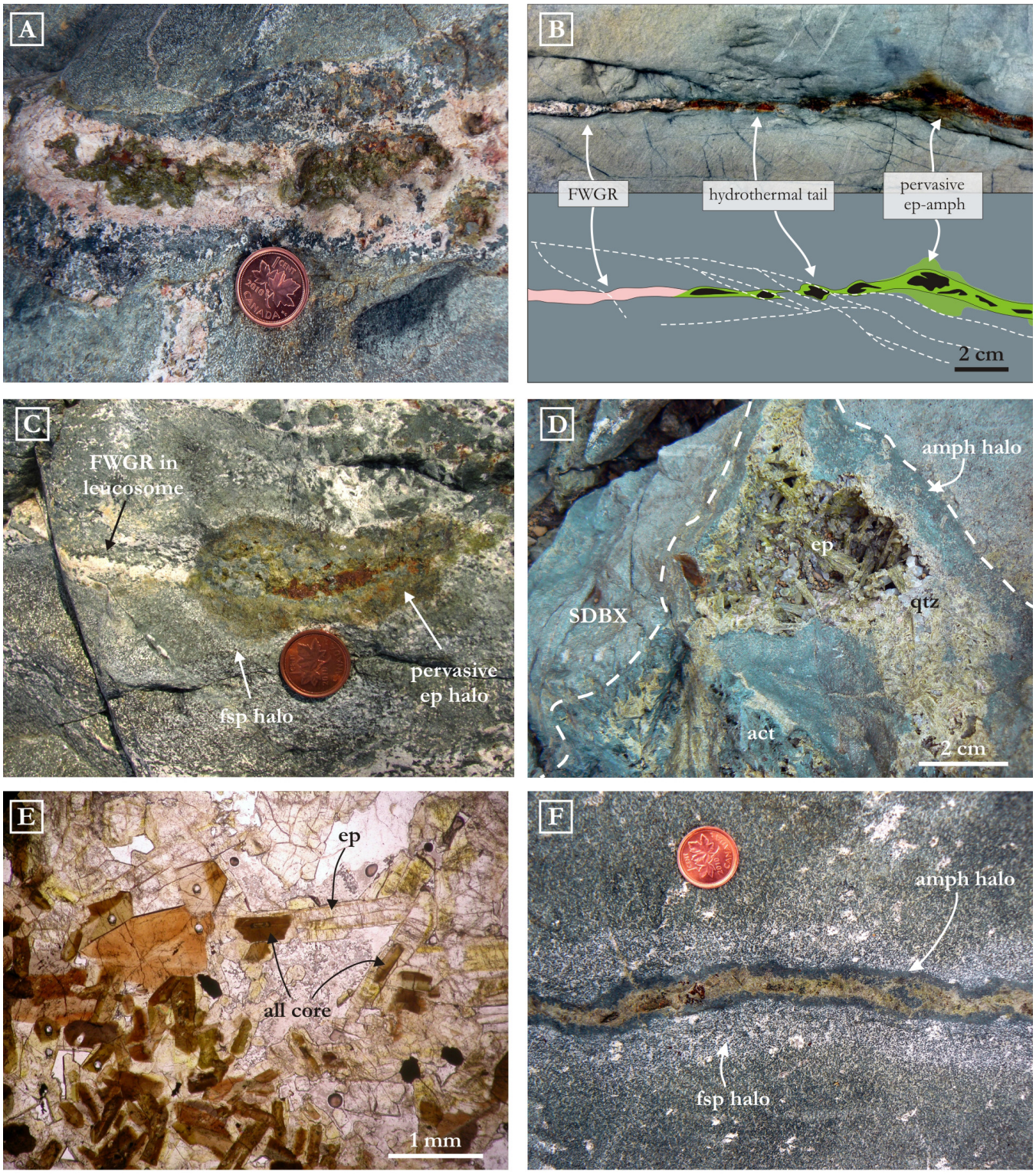

Figure 3. Characteristic macro- and microfeatures of the pre-sulphide assemblages (Amy Lake). **a)** Miarolitic cavity in footwall granophyre, filled by epidote and quartz. **b)** Occurrence of pre-sulphide assemblages in physical contact with footwall granophyre veins: hydrothermal tail and pervasive halo. **c)** Pervasive epidote halo around partially melted leucosome in Levack Gneiss. Note the sulphides in the hydrothermal tail of footwall granophyre and the white feldspar halo around the pervasive epidote. **d)** Pre-sulphide, high-PGE pervasive epidote-amphibole-quartz assemblage in Sudbury Breccia. **e)** Allanite cores in coarse epidote of the pervasive pre-sulphide assemblage (sample 12AV-60). Holes in the grains are ablation pits. **f)** Pre-sulphide epidote vein in mafic gneiss. Note the composite alteration halo. Abbreviations: act = actinolite, all = allanite, amph = amphibole, ep = epidote, fsp = feldspar, FWGR = footwall granophyre, qtz = quartz, SDBX = Sudbury Breccia. Note that the diameter of the coin is 19 mm.

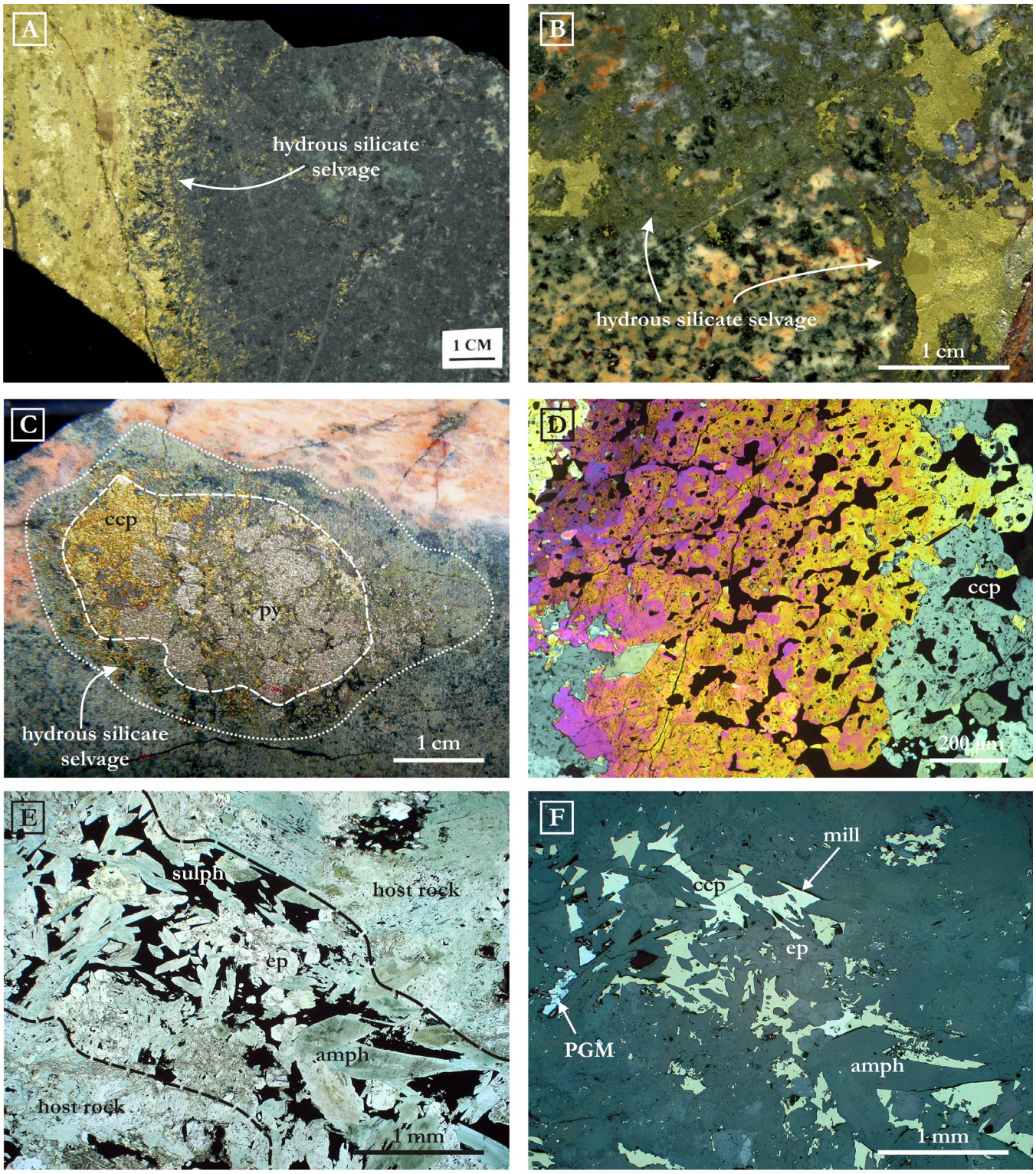

Figure 4. Characteristic macro- and microfeatures of the sulphide-silicate assemblages (footwall mineralization). Silicate selvage around **(a)** massive sulphide veins (Podolsky) and **(b, c)** patchy sulphides from the Wisner Southwest zone (sample 12AV-68) and the Amy Lake PGE zone, respectively. **d)** Poikilitic intergrowth of epidote and chalcopyrite, the characteristic textural feature of footwall mineralization (sample WC-013 173.6). **e, f)** Epidote associated with Ni-rich euhedral actinolite, chalcopyrite, millerite, and PGM in a mineralized sample (WC-013 173.6). Abbreviations: amph = amphibole, ccp = chalcopyrite, ep = epidote, mill = millerite, PGM = platinum-group minerals, py = pyrite, sulph = sulphide.

Extensional amphibole veins occur in both footwall and hanging-wall rocks of the SIC and contain up to 95% acicular actinolite intergrown with minor titanite and, occasionally, with epidote (Fig. 5a). Trace amounts of interstitial K-feldspar and quartz also occur. Amphibole veins exhibit a characteristic white halo of recrystallized albitic feldspar (Fig. 5b). Actinolite veins, 2 cm wide, with pervasive albite-quartz alteration are present in a 3 m wide hanging-wall zone, ~250 m above the upper contact of the SIC, hosted by the equant shard unit, Sandcherry member, Onaping Formation (Ames and Gibson, 2004a) (Fig. 5c,d). Pervasive albite-quartz-titanite zones may be devoid of amphibole or have rims of amphibole. Pervasive amphibole alteration also occurs in veinlets at the terminations of aphanitic andesite dykes in the lower Onaping Formation. This albitization was dated at 1848 ±1 Ma by U-Pb geochronology of titanite (Ames et al., 1998).

Extensional epidote-quartz veins are dominated by coarse epidote and contain variable amounts (up to 25%) of coeval quartz and occasional albite (Fig. 5e) and are found in numerous footwall areas (Wisner West, Amy Lake PGE zone, Broken Hammer, Levack embayment). Large crystals of sperrylite (typically reaching 2–3 mm) are disseminated abundantly in a coarse-grained prismatic epidote and quartz matrix in the Broken Hammer epidote-sperrylite assemblage (Fig. 5f). The alteration completely replaces the gabbroic host rock in an area of about 10 m in diameter in the footwall of the sharp-walled Big Boy sulphide vein (Ames et al., 2013, 2014). The conditions that form these hydrothermal platinum bonanzas are of utmost interest.

Amphibole amygdules

Amphibole is a common alteration mineral in the footwall and hanging-wall hydrothermally altered rocks (Farrow, 1994 and Ames et al., 1998, 2006, respectively). Open-space filling of vesicles with acicular amphibole, allanite, and titanite appear in intensely altered Sudbury Breccia outcrops in the Trill area. The shape and size of these Trill actinolite amygdules are variable, ranging from perfectly round or elongate amygdules of a few millimetres to a few centimetres to oddly shaped patches up to ~20 cm in width (Fig 6a to d). Coarse-grained titanite and zoned allanite are especially abundant filling small vesicles (Fig. 6b,c), whereas large patches have a core of actinolite with minor titanite and allanite along the rim of the amygdule (Fig. 6d). The texture and appearance suggest a fluid was present in the breccia matrix contemporaneous to the deformation of the Sudbury Breccia. Field evidence indicates that this deformation had occurred prior to the formation of extensional epidote-quartz veins in the Trill area.

Above the SIC, in the broad semi-conformable zone of albitization in the lower part of the Onaping Formation, amphibole fills amygdules (Fig. 6e) together with veins with albitized margins (mentioned above); in the most intense albitized-amphibole alteration, it replaces the matrix.

Post-1850 Ma shear-type epidote-quartz veins

Shear-type epidote-quartz veins formed during a regionally widespread post-1850 Ma hydrothermal event involving Ca-Na-Fe-rich moderate-temperature (200–250°C), and high-salinity (33–35 NaCl equiv. wt%) fluids (Tuba et al., 2010, 2014). This hydrothermal assemblage appears in zones and swarms of anastomosing veins, and is dominated by fine- to medium-grained epidote with variable amounts of quartz, chlorite, and occasional hematite. The veins are characterized by a variety of textures that uniformly indicate a shear-related formation (Fig. 7a to d).

RESULTS

As will be discussed later, several factors were found to have influenced the distribution of trace elements in the studied silicates, in some cases causing a large variability of distribution patterns among, and within, samples. For that reason, the authors have picked representative samples when demonstrating the key features of the particular alteration groups (Figs. 8, 11, and 13), whereas all the element distribution diagrams can be found individually in Appendix A (Figs. A1 to A4).

Rare earth element geochemistry of epidote, allanite, amphibole, and titanite

The trace element mineral chemistry data were normalized to the bulk rock geochemistry of the host rock for all data to minimize the influence of host rock (Appendix A, Table A2). Trace element data show that certain rare earth element (REE) patterns are more frequent in some alteration groups, although REE concentrations vary significantly within these groups and, in some cases, even within a given sample. The most useful feature of the host-rock normalized REE plots in the characterization of the alteration groups is the topology of these diagrams, whereas other features (e.g. size of Eu anomaly, level of REE-enrichment of a single mineral) do not show systematic variations. Classification of the alteration groups based on mathematically expressed La:Lu (or other LREE:HREE) ratios was not possible, as individual analyses in heterogeneous samples may scatter over a wide range; therefore the topology of REE plots defined by all analyses in a given sample (typically around 10 ablation spots) was studied. A REE pattern was considered characteristic if it appeared in about 90% of the samples within an alteration group; for that reason,

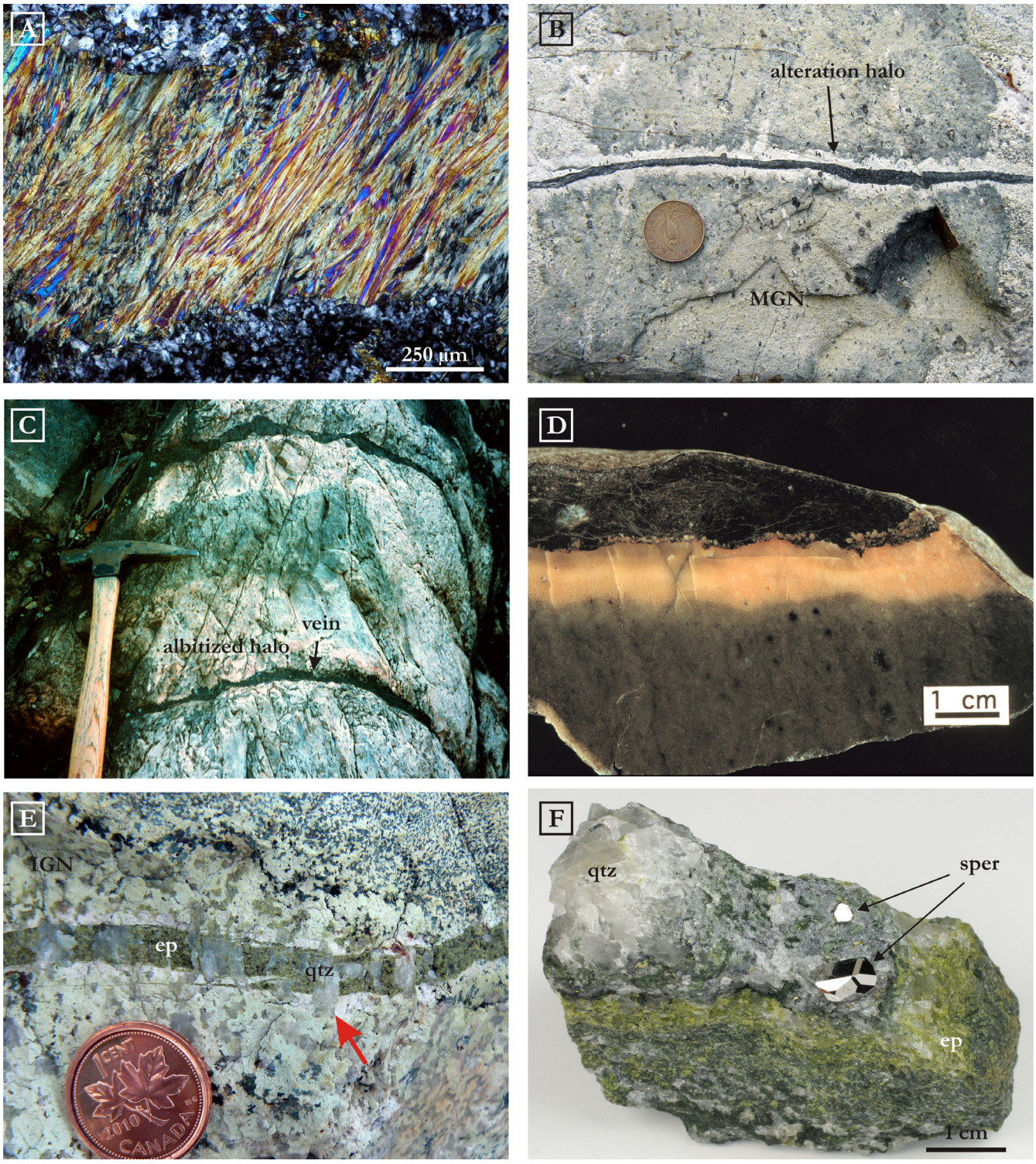

Figure 5. Characteristic macro- and microfeatures of extensional silicate veins and the Broken Hammer epidote-sperrylite assemblage (associated with footwall mineralization). **a)** Photomicrograph of monomineralic, fibrous actinolite filling an amphibole vein (Wisner Southwest). The antitaxial texture is characteristic for all types of silicate veins associated with footwall mineralization. **b)** Amphibole vein in mafic gneiss (Amy Lake). Note the white alteration halo of recrystallized feldspar, similar to that of the pre-sulphide pervasive and vein assemblages. Coin is 21.2 mm in diameter. **c)** Close-up of 1–2 cm actinolite veins and 12–18 cm pervasive albite-quartz alteration haloes within in a 3 m diameter zone proximal to a fluidal breccia sill-dyke complex, Rockcut Lake, Capreol. **d)** Polished slab of actinolite vein and pervasive albite-quartz alteration halo in an equant shard unit, Sandcherry member, Onaping Formation. **e)** Extensional epidote-quartz vein (Wisner Southwest). Note the overgrowth of rock-forming quartz into the vein cavity (red arrow), a typical feature of extensional epidote-quartz veins. Coin is 1.9 cm in diameter. **f)** High-PGE epidote-sperrylite assemblage from Broken Hammer. (Courtesy of Wallbridge Mining Co. Ltd). Abbreviations: ep = epidote, IGN = intermediate gneiss, MGN = mafic gneiss, sper = sperrylite, qtz = quartz.

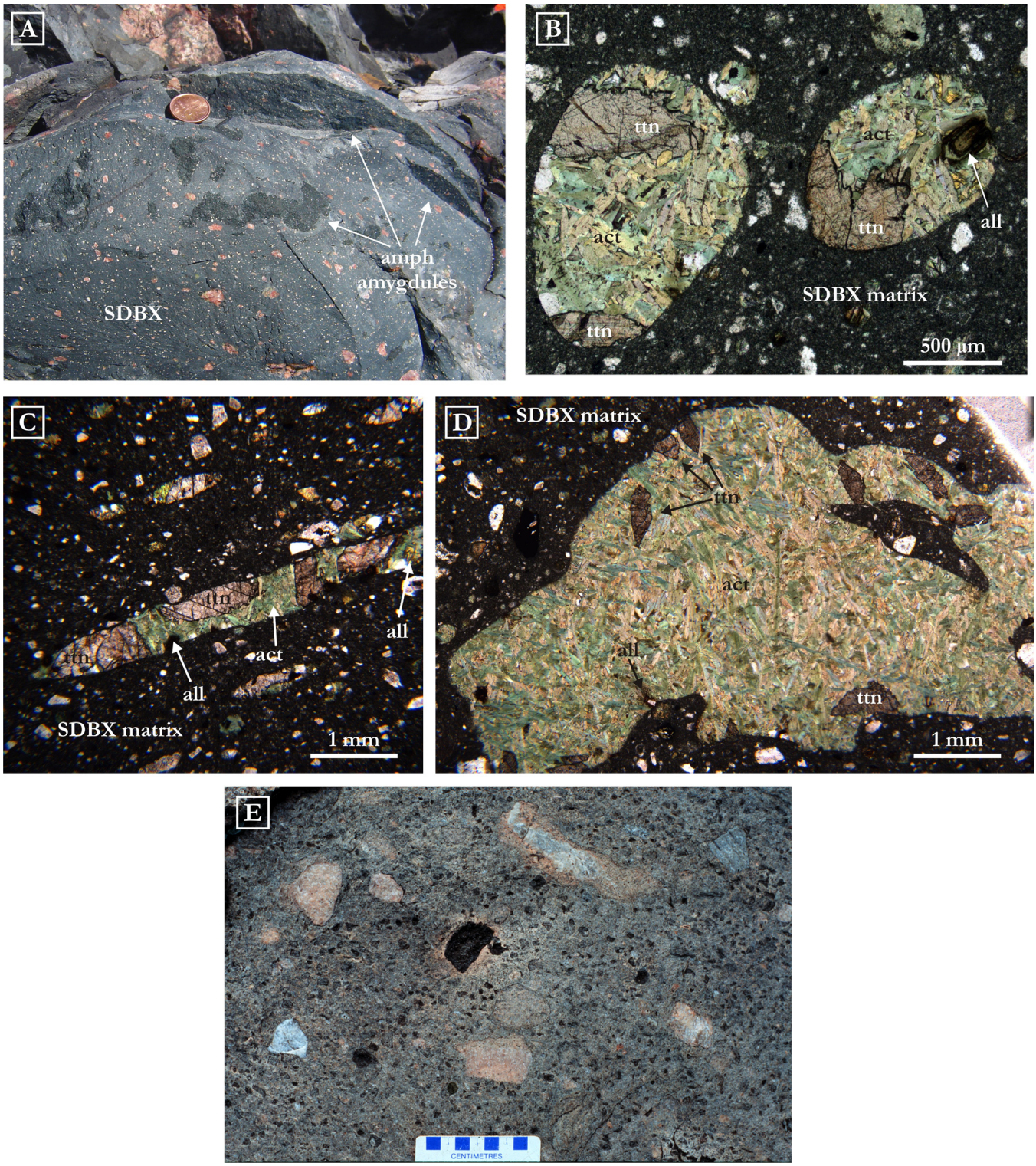

Figure 6. Intense open-space amphibole alteration below and above the SIC occurs as (1) amygdules in Sudbury Breccia (Trill) and (2) amygdules, veins, and stringers in Sandcherry member andesite breccia (Capreol, Joe Lake), respectively. **a)** Outcrop photograph of elongated and irregularly shaped amygdules up to 10 cm in length (Trill). Coin is 1.9 cm in diameter. **b)** Photomicrograph of round amygdules filled with coarse titanite, amphibole (actinolite), and trace allanite (Trill). **c)** Lineation in Sudbury Breccia defined by elongated amygdules (Trill). **d)** Oddly shaped amygdule with a Sudbury Breccia "clast". Note the coarse titanite and allanite located towards the wall of the amygdule. **e)** Intense albitization characterized by partially albitized lithic fragments, matrix, and shards. Shards are actinolite-rich. Actinolite occurs in patches rimmed by albite and vice versa (Joe Lake area). Abbreviations: act = actinolite, all = allanite, amph = amphibole, SDBX = Sudbury Breccia, ttn = titanite).

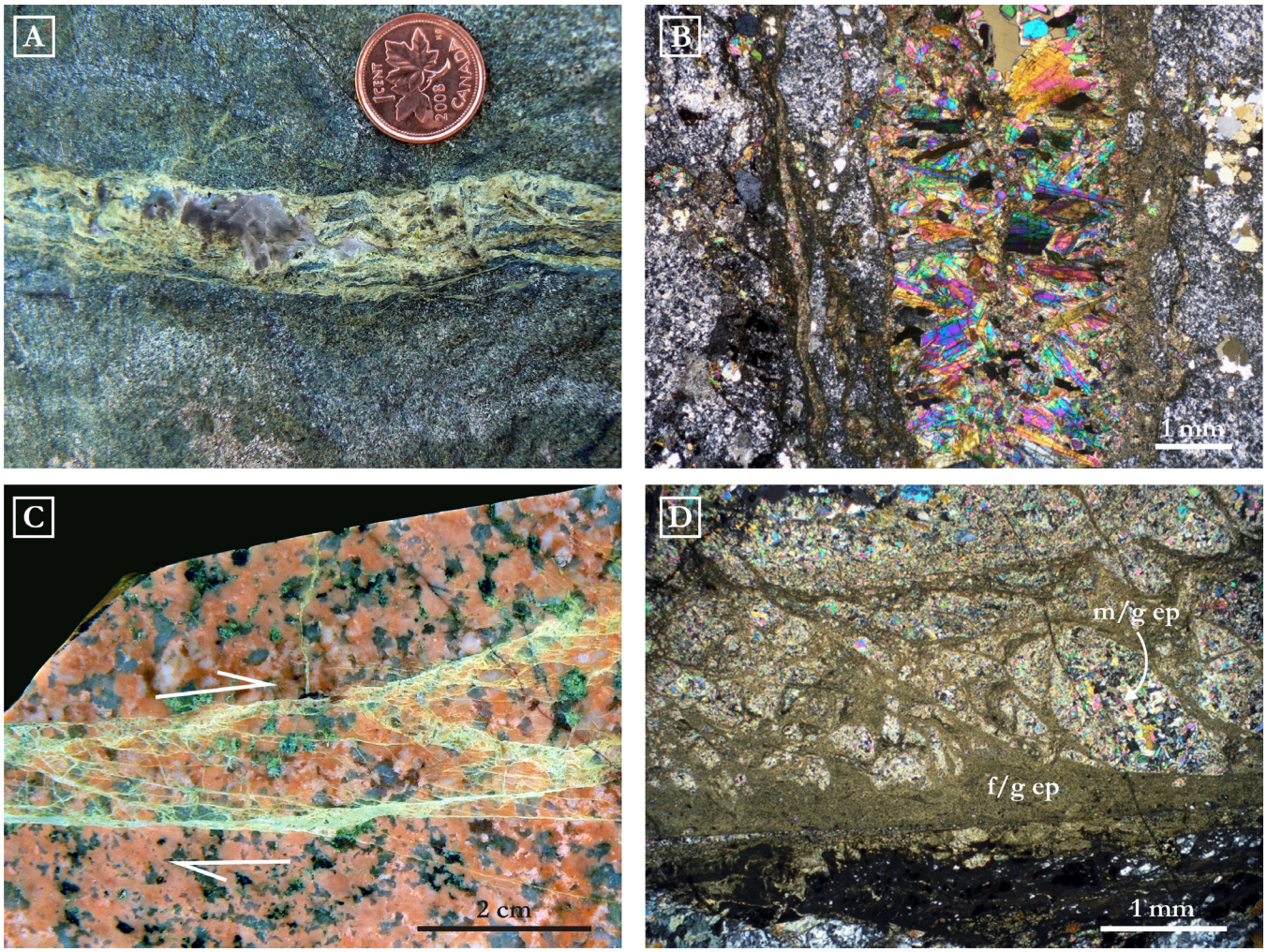

Figure 7. Examples of some of the most common micro- and macro-textures of post-Sudbury shear-type epidote-quartz veins. **a)** Epidote-quartz vein with fluidal texture, cutting gabbro. Width varies along strike. Coin is 1.9 cm in diameter. **b)** Photo-micrograph of the extensional segment of an epidote-filled shear zone. Note the shearing at the margins. Shear indicators (e.g. Riedel structures) in this type of veining often show up at both **(c)** macro- and **(d)** micro-scale. Abbreviations: f/g ep = fine-grained epidote, m/g ep = medium-grained epidote.

miarolitic cavities are not discussed from this aspect, as they were only represented by two samples.

Characteristic rare earth element patterns in epidote and allanite

Epidote in pre-sulphide pervasive and vein-type assemblages are typified by a slightly negative REE trend that shows light REE (nLREE) values are higher than the host-rock normalized heavy REE (nHREE) values (Fig. 8a,b). This negative-slope REE pattern with a positive europium anomaly is characteristic of the pre-ore hydrothermal assemblage and is the key discriminant.

Figure 8 (opposite page). Representative examples of the REE distribution patterns in pre-sulphide epidote, amphibole, and titanite. Typical REE pattern of pre-sulphide in **(a)** pervasive replacement (sample 08AV-05A) and **(b)** vein epidote (sample 12AV-63). The slightly negative trend is characteristic and discriminatory. **c)** Decrease of REE from the allanite core to the epidote rim and prismatic epidote in the pre-sulphide pervasive assemblage (sample 12AV-60). **d)** "Arch-like" REE pattern of poikilitic epidote (sample FAL-12). **e)** REE pattern in extensional epidote is commonly flat with a slight Eu anomaly. The anomaly increases with decreasing concentrations of REE. **f)** A slight increase in Tm, Yb, and Lu is visible in the REE plots of pre-sulphide amphiboles (sample 12AV-60). **g)** Euhedral amphibole from the sulphide-silicate assemblage is usually low in REE and shows large intra-sample variations in some cases (sample 11AV-62F). **h)** Typical REE pattern of extensional amphibole from both the footwall (sample BLT-05) and hanging wall (sample AV-488B) of the SIC show a similar topology to the **(i)** actinolite in hanging-wall amygdules (sample AV-524A), as they are all mono-mineralic assemblages. This is in contrast to the amphibole assemblage with allanite and titanite in the footwall amygdules (sample 604054), where amphibole is depleted in LREE. **j)** REE in titanite decreases from the miarolitic cavities (sample 12AV-57) to pre-sulphide epidote veins (sample 12AV-63) and extensional amphibole veins (sample 12AV-78). (Titanite from Trill amygdules and Onaping amphibole veins are not shown to avoid overlapping; refer to text, and Appendix A, Fig. A4 for individual charts.)

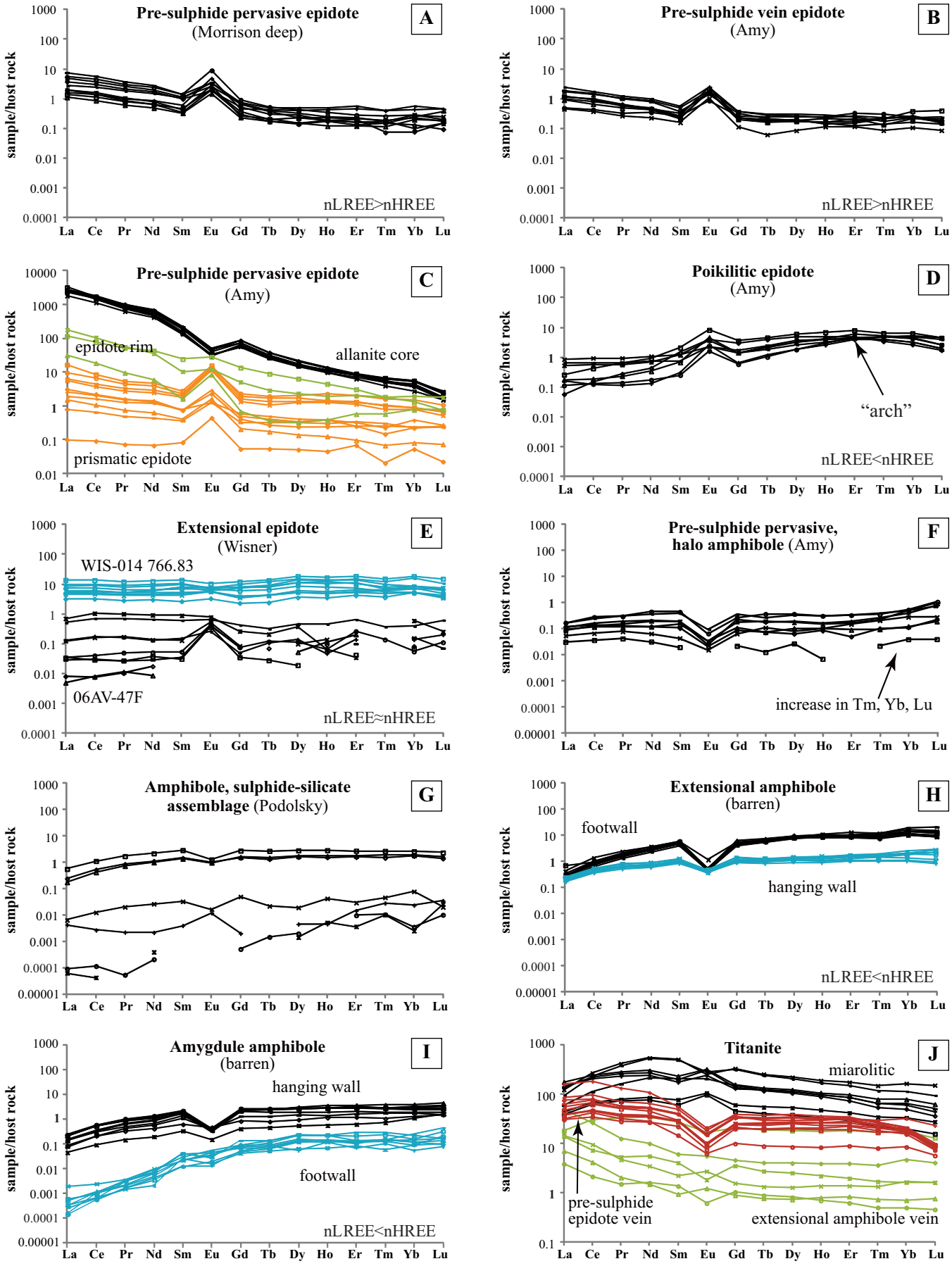
A
Pre-sulphide pervasive epidote
(Morrison deep)
nLREE>nHREE
B
Pre-sulphide vein epidote
(Amy)
nLREE>nHREE
C
Pre-sulphide pervasive epidote
(Amy)
epidote rim
allanite core
prismatic epidote
D
Poikilitic epidote
(Amy)
"arch"
nLREE<nHREE
E
Extensional epidote
(Wisner)
WIS-014 766.83
06AV-47F
nLREE≈nHREE
F
Pre-sulphide pervasive,
halo amphibole (Amy)
increase in Tm, Yb, Lu
G
Amphibole, sulphide-silicate
assemblage (Podolsky)
H
Extensional amphibole
(barren)
footwall
hanging wall
nLREE<nHREE
I
Amygdule amphibole
(barren)
hanging wall
footwall
nLREE<nHREE
J
Titanite
miarolitic
pre-sulphide
epidote vein
extensional amphibole vein
sample/host rock
La Ce Pr Nd Sm Eu Gd Tb Dy Ho Er Tm Yb Lu

Allanite cores are present in epidote within pervasive epidote-amphibole alteration (Fig 3e). They contain approximately 16 wt% REE (5.5 wt% La, 8.0 wt% Ce, 0.7 wt% Pr, 2.0 wt% Nd, and 0.1 wt% Sm in average) whereas the total REE content of prismatic epidote is below 700 ppm (Appendix A, Table A3). There is a gradual decrease in the REE concentrations and a systematic increase in the Eu anomaly (from negative to flat to positive) from the allanite cores to the epidote rims and coarse prismatic epidote (Fig. 8c; Appendix A, Fig. A1).

The coarse allanite in the amygdules within Sudbury Breccia in the Trill area (Fig 6a,b) is enriched in LREE with a total average REE content of ~7.8 wt% (2.0 wt% La, 3.8 wt% Ce, 0.4 wt% Pr, 1.4 wt% Nd, and 0.2 wt% Sm), and has a flat nLREE and negative nHREE trend (Appendix A, Table A3, Fig. A1).

Epidote in the mineralization-related hydrothermal assemblages is typically poikilitic with inclusions of anhedral chalcopyrite, PGMs, and base metal minerals such as galena and cassiterite (White, 2010; Tuba et al., 2010, 2014; Ames and Kjarsgaard, 2013). The epidote REE pattern has a slightly positive slope, a Eu anomaly that varies significantly within sample between positive and negative and a slight arch in the nHREE. Normalized LREE is equal to or, more commonly, depleted compared to nHREE. The ore-associated poikilitic epidote exhibits large intra-sample variation in nLREE and more consistent nHREE values; this results in an arch-like REE topology (Fig. 8d; Appendix A, Fig. A2).

Sulphide-free extensional epidote observed in various localities is usually enriched in both LREE and HREE with a flat REE trend and a slightly negative to absent Eu anomaly that is quite consistent within the sample. An increase in the size of the positive Eu anomaly can be observed in samples with lower nREE concentrations (Fig. 8e). Extensional epidote veins from the Broken Hammer sperrylite zone have a REE topology that is more similar to those of the poikilitic epidote in the sulphide-silicate assemblage, whereas the sperrylite-accompanied coarse epidote (sample 12AV-18x) shows a flat, slightly positive nREE pattern that resembles the nREE distribution of extensional epidote veins (Appendix A, Fig. A2).

Rare-earth element ratios, concentrations, and trends are quite variable in the post-Sudbury shear-type epidote group and distinct features could not be convincingly established (Appendix A, Fig. A2).

Characteristic rare earth element patterns in amphibole

Mineral compositions of three textural types of amphibole from pre-sulphide assemblages were analyzed: 1) amphibole intergrown with coarse prismatic epidote within pervasive epidote-amphibole alteration zones, 2) amphibole in the halo of pervasive epidote-amphibole alteration, and 3) amphibole in the halo of the vein-type epidote alteration. Regardless of the textural position, all of the amphiboles in this alteration group are uniformly low in REE, have a negative Eu anomaly, and a flat REE trend with a slight inclination in Tm, Yb, and Lu (Fig. 8f; Appendix A, Fig. A3).

Amphibole along the margins of chalcopyrite-PGM veins, in the mineralization-related sulphide-bearing hydrothermal alteration, is typified by low overall REE concentrations and a generally flat trend with a small negative Eu anomaly (Fig. 8g). Similar to poikilitic epidote, the largest variation of REE concentration in amphibole, both within and among samples, was observed in this group (Appendix A, Fig. A3).

Barren extensional amphibole veins and amphibole in amygdules from both the footwall and hanging wall of the Sudbury Igneous Complex are characterized by similar REE distribution features (Fig. 8h,i): an overall positive REE trend with an inclination in nLREE, flat nHREE, and a pronounced negative Eu anomaly. REE concentrations of amphibole grains within these samples are usually very homogeneous (Appendix A, Fig. A3).

Rare earth elements in titanite

Rare-earth element concentrations in titanite decrease from grains in miarolitic cavities (0.9 wt% average total REE) to 1848 Ma grains in the Onaping alteration haloes (0.5 wt%), pre-ore veins (0.3 wt%), and to titanite intergrown with actinolite in extensional amphibole veins and Trill amygdules (0.2 and 0.1 wt%, respectively) (Fig. 8j; Appendix A, Table A5, Fig. A4). Uranium and Th in titanite seem to follow the same trend. Because of the reduced number of samples available for titanite trace element study, the key features in the topology of REE plots representing the different alteration groups could not be determined.

Pathfinder and other trace elements in epidote, allanite, and amphibole

Lead and Ni proved to be the best candidates in epidote for classifying the alteration groups (Fig. 9a,b). The topologies of the Pb versus Ni diagrams are very similar regardless of the values plotted (absolute concentrations in ppm or host-rock normalized values; Fig. 9a and b, respectively), suggesting that the concentrations of these elements are not a function of host-rock composition but rather of fluid composition. Epidote-bearing assemblages predating the sulphide mineralization are dominantly lower in Pb (<5 ppm) than those associated with the sulphide-bearing system, although the two groups overlap slightly. Among the pre-sulphide assemblages, Ni is lowest (<1 ppm) in the miarolitic epidote, and highest (typically a few 100 ppm) in the

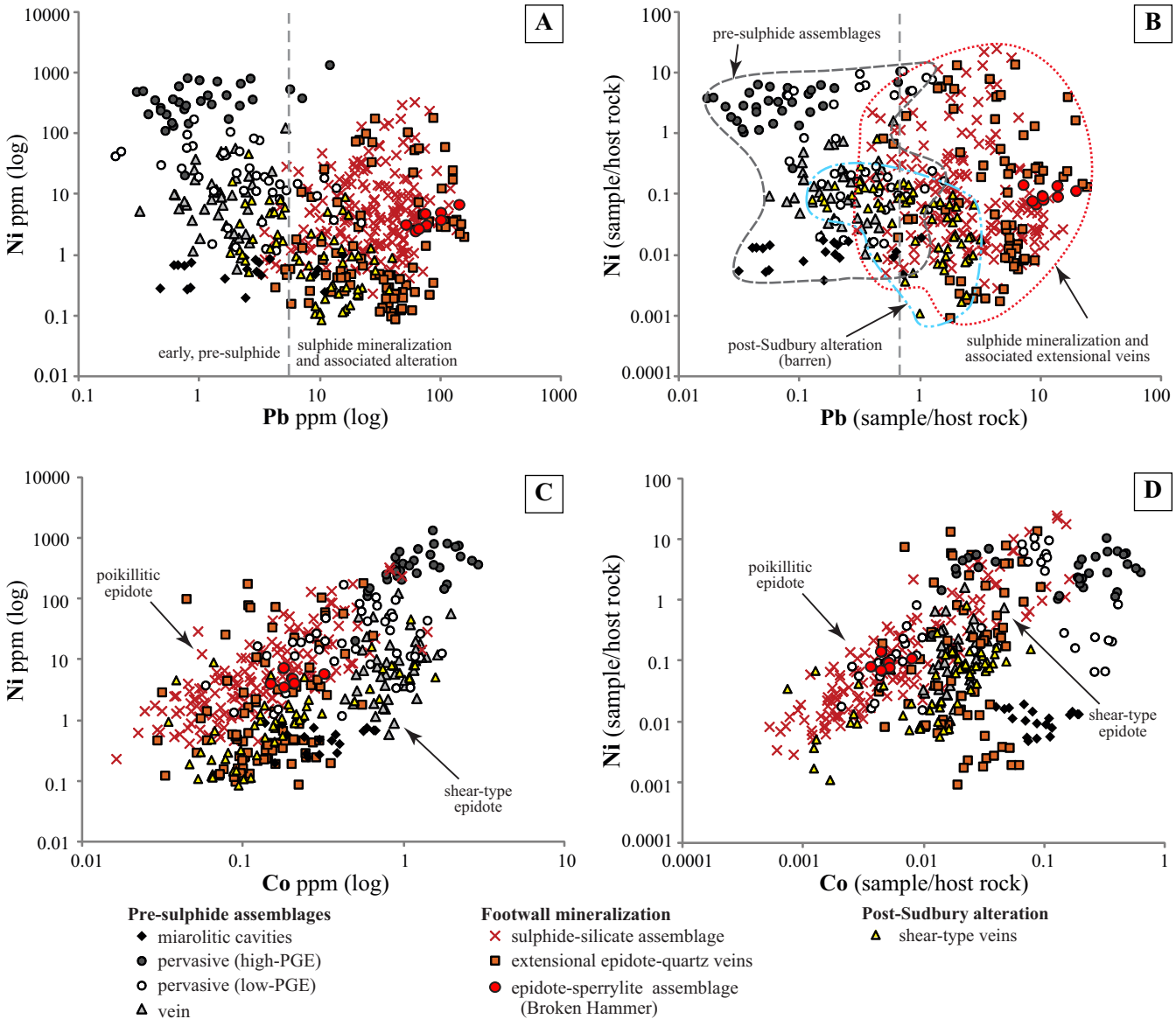

Figure 9. Select pathfinder elements in epidote. Note logarithmic scale. **a)** Absolute and **(b)** host-rock normalized concentration of Pb and Ni. Pre-sulphide assemblages may be distinguished from those associated with footwall mineralization based on the lower Pb content. Post-Sudbury shear-type veins overlap with both groups. Among pre-sulphide assemblages, high-PGE pervasive epidote samples show the highest Ni values. **c)** Absolute and **(d)** host-rock normalized concentration of Co and Ni. Note the difference in the topology of the two plots indicating an effect of host rock on Co concentration in certain assemblages. Co and Ni correlates well in poikilitic epidote.

high-PGE pervasively epidotized alteration. Vein-type epidote and most of the low-PGE pervasive epidotes plot in-between. Nickel content in poikilitic epidote of the sulphide-silicate assemblage and in extensional veins ranges widely (0.1–300 ppm). Although the pre-sulphide and sulphide-bearing systems may be distinguished based on the Pb content of epidote; the Pb and Ni values of epidote in post-Sudbury shear-type veins overlap with both groups. The observations regarding Pb and Ni patterns as discussed above are generally in agreement with the findings of Tuba et al. (2014).

A positive correlation previously found between Co and Ni in epidote (Tuba et al., 2014) does not show clearly in this extended database. Comparison of Figure 9c and 9d shows that the host-rock composition may have influenced the concentration of Co in most alteration assemblages. Only the shear-type and poikilitic epidote samples do not show a major change in the topology of Co versus Ni plots; however, a strong positive correlation does occur in poikilitic epidote, suggesting a link between these elements in the fluids associated with footwall mineralization.

Allanite cores of pre-sulphide pervasive assemblages are depleted in Pb but enriched in Ni, compared to allanite in the sulphide-free Trill amygdules (Fig. 10). A possible explanation could be that Trill amyg-

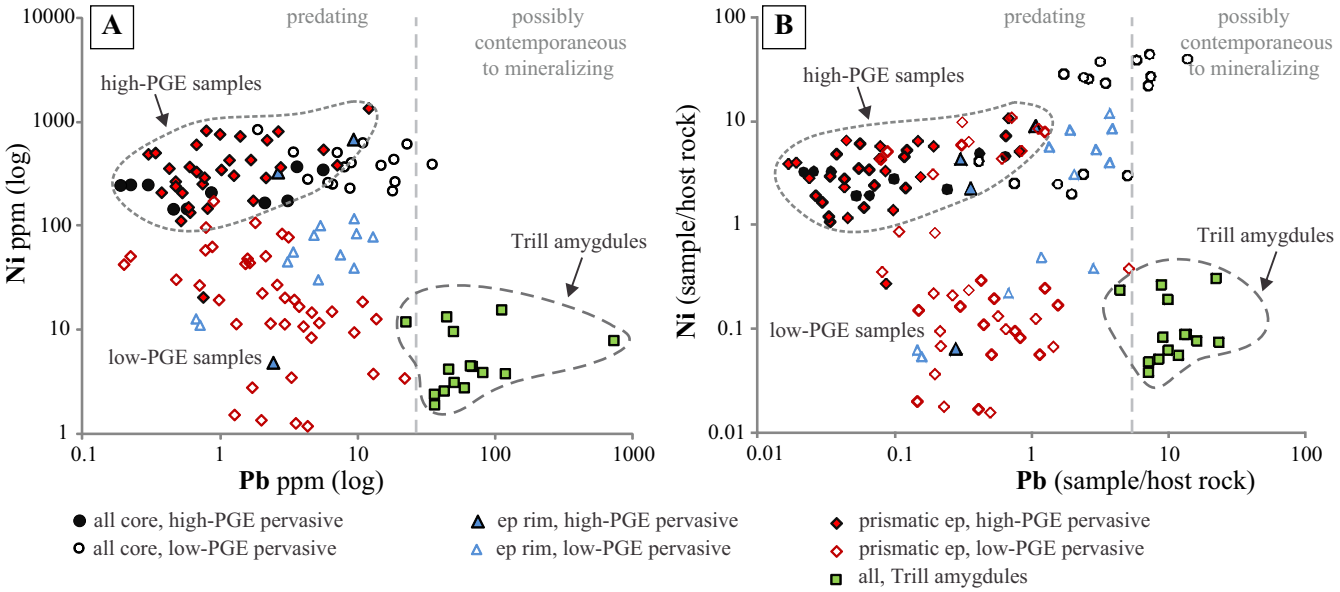

Figure 10. Concentration of **(a)** Pb and **(b)** Ni in pre-sulphide assemblages and amygdules in Sudbury Breccia, Trill property. (Note the logarithmic scale.) High-PGE samples are generally higher in Ni than low-PGE samples, whereas Pb is enriched in Trill amygdules. Enrichment of Pb suggests a possible genetic link with the Sudbury-related, potentially mineralizing hydrothermal fluids. Abbreviations: all = allanite, ep = epidote.

dules represent barren hydrothermal cells that were similar to the mineralizing fluids (resulting in the high-PGE sulphide-silicate assemblages) but lacked a local base metal source. Although allanite cores in pervasive epidote alteration uniformly contain a few 100 ppm Ni, the epidote rims and prismatic epidote associated with high-PGE alteration are enriched compared to those in low-PGE pervasive assemblages (Fig. 10).

The three allanite-bearing, pervasive pre-sulphide samples uniformly show a decrease of Co, Zn, As, Mg, Ti, Cr, Y, Th, and U, as well as an increase of Sr from the allanite core to the epidote rim and coarse prismatic epidote (Fig. 11). Nickel decreases in low-PGE samples only, whereas in high-PGE samples it is equally distributed in allanite and epidote (Fig. 10). Tin and Sb are present in roughly identical values in allanite and epidote and other elements vary.

Amphibole-bearing assemblages may be fingerprinted based on their Ni and Sn content (Fig. 12a,b). Pre-sulphide, pervasively altered assemblages associated with high PGE content contain the highest amounts of Ni (0.2 wt% Ni average) in both the amphibole that occurs with prismatic epidote and the amphibole that forms the finer grained actinolite halo around the pervasive alteration (Fig. 3d,e). The actinolite halo around pre-sulphide epidote veins, as well as amphibole amygdules are both Ni-poor (<300 ppm).

Euhedral amphibole in sulphide-silicate assemblages in the footwall mineralization is enriched in Ni with values ranging from >0.1 to 1 wt% Ni. Such high concentration of Ni in this type of amphibole is widely known to occur in the Sudbury footwall (Farrow, 1994; Farrow and Watkinson, 1996; Magyarosi et al., 2002; Kjarsgaard and Ames, 2010; Tuba et al., 2010, 2014). Unmineralized extensional amphibole veins fall into the low-Ni area of the diagrams, typically with 100 to

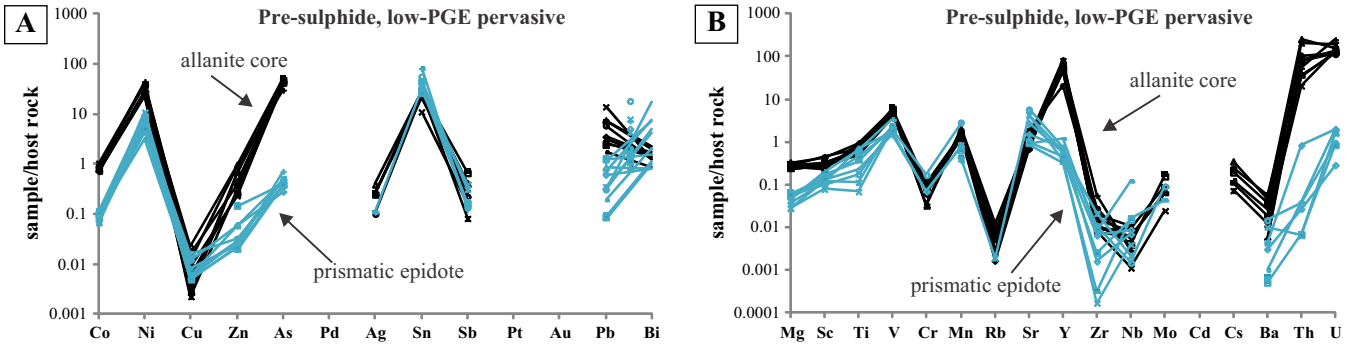

Figure 11. Trace element signatures in allanite and epidote (sample 11AV-57) showing the distribution of **(a)** pathfinder and **(b)** other trace elements between allanite cores and prismatic epidote in the pre-sulphide pervasive epidote-amphibole assemblage. Cobalt, Zn, As, Mg, Ti, Cr, Y, Th, and U concentrations are markedly different in the two mineral phases.

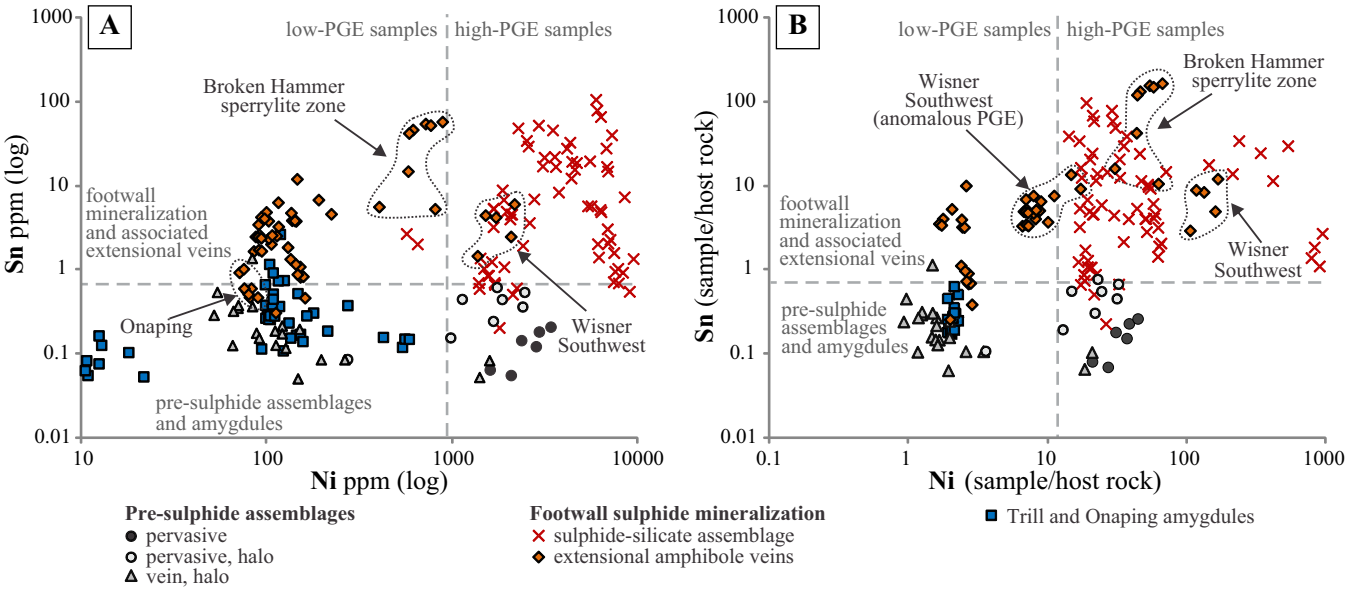

Figure 12. Trace element signatures in amphibole. **a)** Absolute and **(b)** host-rock normalized Ni and Sn concentration in amphibole. (Note logarithmic scale.) Ni is enriched in high-PGE assemblages (high-PGE pervasive pre-sulphide assemblage, sulphide-silicate assemblage of footwall mineralization and some anomalously high-PGE extensional amphibole veins), whereas Sn concentration is dominantly higher in amphiboles from footwall mineralization and associated extensional veins. (Note that normalized values of extensional amphibole veins and amphibole amygdules from the Onaping Formation are not available due to the lack of Sn analyses from the host rock.)

200 ppm Ni; among them, two samples (BLT-03 and BLT-05) with anomalous bulk PGE contents (0.01 ppm: Tuba, 2012) plot close to the high-PGE field. The Ni content of amphibole in high-PGE extensional veins (samples 12AV-15B and BLT-06) is typically 0.04 to 0.1 wt%. Nickel content in extensional amphibole as a function of bulk total precious metal content and/or proximity to footwall mineralization had previously been documented by Hanley and Bray (2009) and Tuba et al. (2010). Tin is also enriched (>1 ppm) in sulphide-silicate assemblages and extensional veins in footwall ore systems, whereas concentrations of Sn in the extensional amphibole veins from the hanging wall (Onaping Formation) are below 1 ppm, in the upper section of the low-Sn group that also contains the pre-sulphide assemblages and amphibole amygdules from both the footwall and hanging wall.

Table 4. Summary of the systematic element partitioning between coexisting minerals.

	REE and pathfinder elements	Other trace elements
Epidote-amphibole		
ep>amph	REE, Pb, Bi, Sn	Sr, U
amph>ep	Co, Ni, Zn	Mn, Rb
ep~amph	As	
Based on 12 samples representing 4 alteration groups. Observed frequency of given element distribution among mineral pairs: minimum 90%.		
Titanite-amphibole		
ttn>amph	REE, Sn, Bi	V, Y, Zr, Nb, Mo, Th, U
amph>ttn	Co, Ni, Zn	Sc, Mn, Ba
ttn~amph	Cu	Rb
Based on 4 samples representing 2 alteration groups. Observed frequency of given element distribution among mineral pairs: 100%		
Titanite-epidote		
ttn>ep	REE, As, Sn, Pb	Sc, V, Cr, Y, Zr, Nb, Mo, Th, U
ep>ttn	Co	Mn, Sr
ttn~ep	Zn, Sb	Mg, Ba
Based on 2 samples representing 2 alteration groups. Observed frequency of given element distribution among mineral pairs: 100%. For informational purposes only.		

Abbreviations: amph = amphibole, ep = epidote, ttn = titanite.

Elements that occur with concentrations close to the detection limit of the ICP-MS in both minerals included Ag, Sb, Pt, Au, Bi, Mo, Rh, Cd, Cs. Other elements usually detected in very low concentrations regardless of the alteration type include Pd and Bi in epidote. Copper varies greatly and unsystematically. Clear systematic variation of other trace elements was not found in either the epidote or the amphibole sample suite.

DISCUSSION

Factors affecting the trace element distribution patterns in epidote, actinolite, titanite, and allanite

Element partitioning between minerals

With the systematic analysis of all major and minor mineral phases in the alteration assemblages, it was possible to highlight certain partitioning behaviour of trace elements between hydrothermal minerals that are

in apparent petrographic equilibrium (Table 4). These observations are of major significance for characterizing the trace element properties of the respective fluid systems that the alteration assemblages represent, and also highlight important aspects to be considered in detailed trace element studies in the future.

Trace element partitioning between epidote and amphibole, the two most common alteration minerals in the Sudbury footwall, proved to be an important feature. In 12 samples with coexisting epidote and amphibole, As is distributed equally between the two minerals. In addition, epidote appears to have scavenged REE, Pb, Bi, and Sn from amphibole, whereas amphibole is significantly enriched in Co, Ni, and Zn (Table 4, Fig. 13a to c). The systematic distribution of REE was observed in all of these samples, and over 90% of the samples showed the same partitioning of the pathfinder elements. Copper prefers amphibole or is distributed equally between the two minerals, whereas Pd and Ag are never enriched in amphibole. The behaviour of Sb was found to be erratic.

This partitioning phenomenon has a significant effect on the topology of REE plots, and, in fact, may be an explanation for some REE patterns that differ pronouncedly from the average, most frequent REE patterns of the same alteration group. The typically low-REE content of euhedral actinolite in the mineralized sulphide-silicate assemblage is likely due to the scavenger behaviour of the poikilitic epidote with which the amphibole is associated (Fig. 13a). Similarly, in amphibole-dominated, essentially monomineralic assemblages (e.g. extensional actinolite veins and Onaping amygdules) the amphibole is the main REE-bearing phase, and is significantly more enriched in REE than the amphibole occurring with epidote, titanite, or allanite in other assemblages (e.g. note the depletion of nLREE in amphibole in allanite- and titanite-bearing Trill amygdule samples compared to monomineralic Onaping amphibole amygdules in Fig. 8i).

Figure 13d and e demonstrates the scavenging effect of epidote on the sample scale: two extensional amphibole veins, the monomineralic sample BLT-03 and the minor epidote-bearing sample BLT-06, are being compared. The REE-depleted amphiboles located in the vicinity (i.e. less than a few mm distance) of epidote grains have distinctively different REE concentrations and pattern to the amphibole in epidote-free areas of the same sample and amphibole in the non epidote-bearing BLT-03 vein (Fig 13e).

Element partitioning between titanite and amphibole as well as titanite and epidote was studied with a smaller data set. Four samples representing three alteration groups (miarolitic cavities, extensional amphibole veins, and amygdules in Sudbury Breccia from Trill) showed that trace element partitioning is most pronounced in the concentration of REE, Sn, Zr, Nb, Yb, Th, and U (affinity to titanite) as well as Co, Ni, and Zn (affinity to amphibole) (Fig. 13f to h). Table 4 summarizes all the observed systematic trace element distributions.

As discussed in the previous section, although epidote is by far the most common alteration mineral in the Sudbury footwall alteration assemblages, the epidote trace element plots should always be viewed in context to the composition data of other major and minor mineral phases in the alteration assemblage (if applicable).

Crystal structural control and the effect of country rocks

Certain elements correlate well at the database scale (e.g. Ti and Zr in amphibole, Fig. 14a) and/or on the sample scale (e.g. Co and Ni, Fig. 14b), although they do not define systematic distribution patterns among the alteration assemblages. Element substitution phenomena in these minerals are likely responsible for a number of these correlations; however, pinpointing these is problematic due to the difficult coupled substitution mechanisms in both epidote and amphibole and the large number of trace elements to be considered. Some differences between the composition of allanite cores and prismatic epidote in pervasive pre-sulphide samples are probably due to structural reasons, e.g., the decrease of Mg and increase of Sr with decreasing REE; depleted Y, U, and Th content in epidote may be explained by changes in fluid composition because of the shared occupancy of these elements and REE in the epidote structure (Frei et al., 2004).

The role of fluid-rock interaction in the formation of pre-sulphide, sulphide-silicate and, particularly, the extensional assemblages is significant (Tuba et al., 2014). The host rock may add elements to the hydrothermal fluid that could affect the composition of minerals at the trace level; for that reason, trace elements, especially those with low concentrations in a mineral, may show a diversity in a given alteration group that reflect the heterogeneity of country rocks rather than the heterogeneity of fluids. Consequently, all absolute element concentrations are normalized to the respective host rock and the two values are discussed in context, in order to eliminate such fluid-rock effects at the ppm level. Normalization of the data does not usually result in any major differences between the topology of the two diagrams, the one showing the absolute and the other the normalized values, instead it just “tightens up” the samples within the groups by removing outliers. As such, the relative position of the groups generally does not change much but where it does, it likely indicates that fluid-rock interaction had

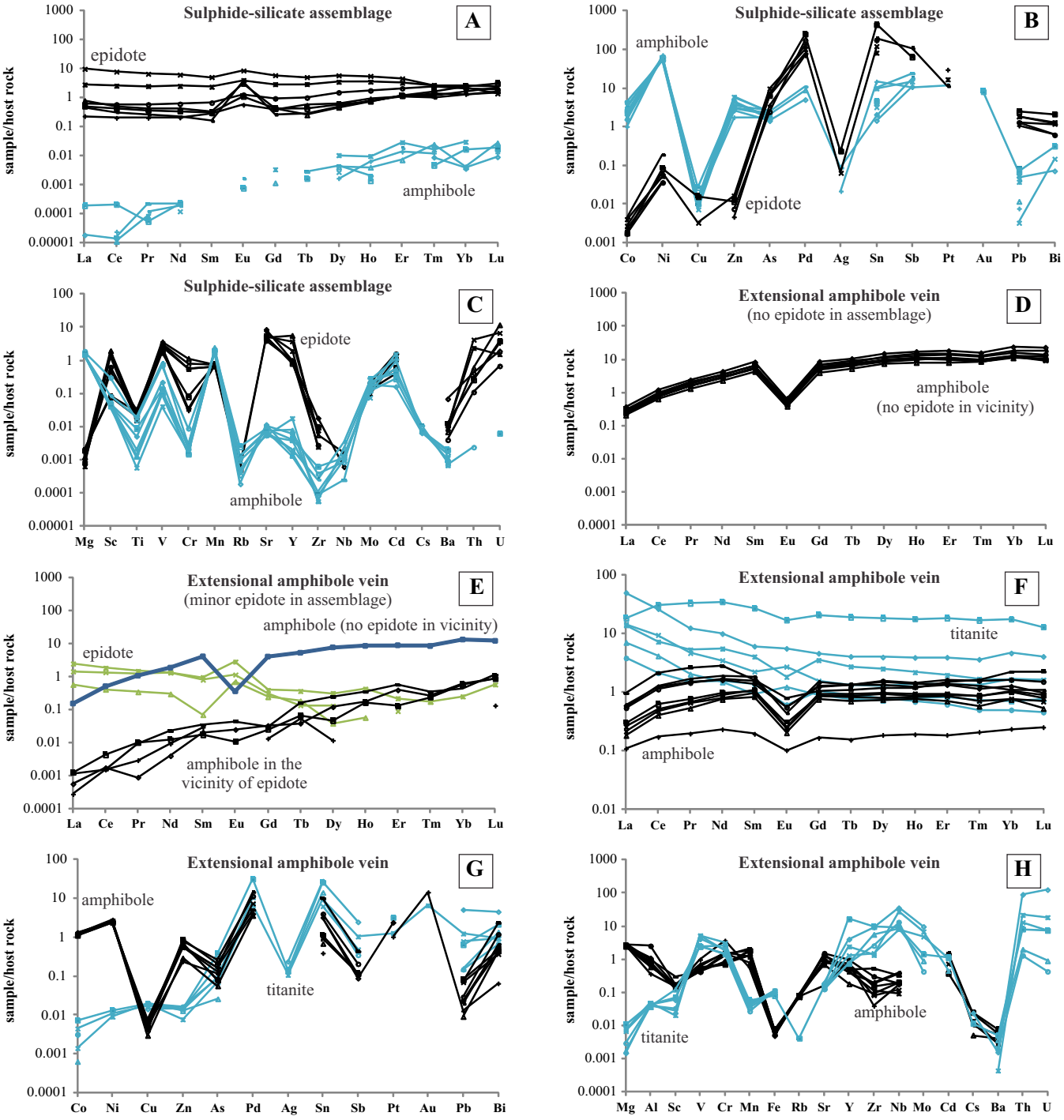

Figure 13. Distribution of trace elements among coexisting minerals normalized to host rock. Partitioning of **(a)** REE, **(b)** pathfinder and **(c)** other trace elements among epidote (black) and amphibole (blue) (sample 02AV-642, sulphide-silicate assemblage). Similar scavenging phenomenon between epidote and amphibole was found in 11 additional samples. **d)** Amphibole in an extensional vein with no epidote in the assemblage (sample BLT-03). Compare REE pattern with that of sample BLT-06 **(e)**, where amphibole in the vicinity of epidote is depleted in REE, whereas amphibole from a different area of the sample shows identical patterns to epidote-free sample BLT-03. **f)** Partitioning of REE, (**g)** pathfinder, and **(h)** other trace elements among amphibole (black) and titanite (blue) (sample 12AV-78, extensional amphibole vein). See text for details.

an impact on certain alteration assemblages. For example, normalizing the As in epidote results in a significant shift of poikilitic samples while others preserve their relative position (Fig. 14c,d), suggesting that As in the sulphide-silicate assemblage is at least partly dependent on the host rock. Plotting these samples according to geographic locations results in a low-As group, which includes the Onaping-Levack area, and a high-As group from Wisner, Podolsky, and Amy Lake, where elevated As concentrations have been reported

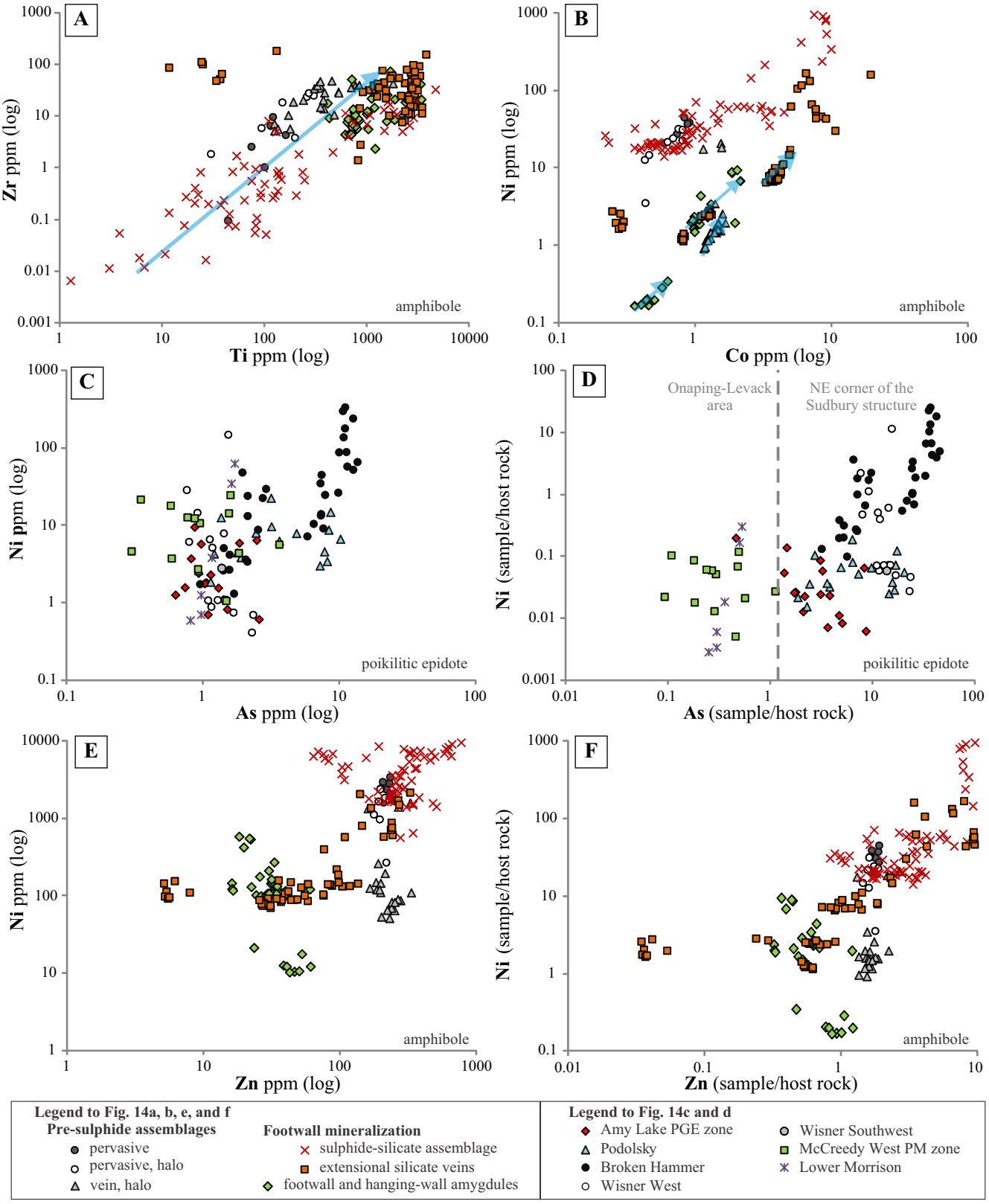

Figure 14. Selected element ratios suggesting the effect of crystal structural and/or host-rock composition control on the trace element distribution of the studied silicates. **a)** Positive correlation of Ti and Zr in amphibole on the database scale, and **(b)** Co and Ni on the sample scale (indicated by arrows). **c)** Absolute and **(d)** host-rock normalized As and Ni content of poikilitic epidote. Based on the significant difference between the two diagrams, fluid-rock interaction likely affected the As concentration of the parental fluid in these samples. Host-rock normalized As is lower in samples from the Onaping-Levack area, where no mafic units are known to occur in large volumes. **e)** Absolute and **(f)** host-rock normalized Zn and Ni concentrations in amphibole. It is likely that Zn was affected by host-rock composition as well, especially in the sulphide-silicate assemblage.

and linked to the local mafic units (Ames et al., 2007; Péntek et al., 2008; Tuba et al., 2014). A similar phenomenon was observed in the concentration of, e.g., Zn, for which mineralized and extensional samples shift significantly once normalized to host rock (Fig. 14e and f), suggesting that both As and Zn are host-rock dependant in these alteration types.

Trace element composition of the alteration assemblages

In a recent study, the REE content of epidote-bearing alteration assemblages in the Amy Lake zone of the Sudbury footwall was linked to a possible magmatic fluid component that mixed with local saline groundwater (Tuba et al., 2014). For this model, only epidote and allanite trace element data were available, and the authors assumed that coexisting minerals, e.g., titanite, may also be reservoirs for REE. The present study contains supplementary data for these potentially REE-bearing minerals and extends the investigation to other localities and alteration types throughout the Sudbury hydrothermal system above and below the SIC.

A systematic variation in the overall REE content of the alteration assemblages, as shown by Tuba et al. (2014), is robust with a larger, diverse data set (Fig. 15). Miarolitic cavities and pervasive epidote-amphibole alteration were associated with minerals bearing the highest concentrations of REE (titanite and allanite, respectively). Allanite and titanite in the Trill amphibole amygdules have similar REE contents to the titanite in pre-sulphide epidote veins, although the bulk REE content of the whole amygdule assemblage is likely much higher than that of the pre-sulphide veins due to the significantly higher amount of titanite and allanite found in the Trill samples. Rare-earth element content in titanite decreases further from pre-sulphide epidote veins to mineralization-related extensional actinolite veins. Epidote is the main REE-carrier in extensional epidote veins, mineralized sulphide-silicate assemblages, and late shear-type veins; these assemblages are generally low in REE, although extensional epidote and actinolite veins from the vicinity of

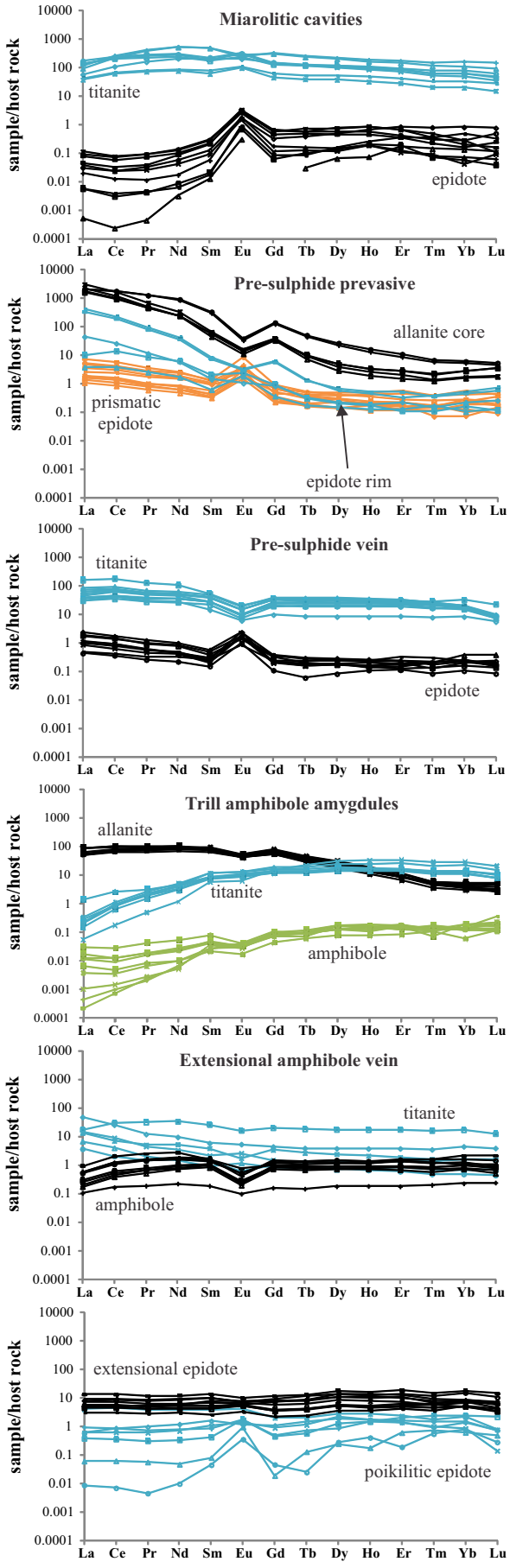

Figure 15. Representative REE plots of alteration assemblages (shown in paragenetic order from top to bottom; Note that the position of the Trill amygdules in the paragenetic sequence is equivocal). The diagrams present the main reservoir minerals for REE (where applicable). A gradual decrease in bulk REE can be observed with higher REE concentrations associated with pre-sulphide assemblages (pervasive: sample 08AV-05A, vein: sample 12AV-63) and low REE being typical for footwall mineralization systems (poikilitic epidote: sample 06AV-37A, extensional amphibole vein: sample 12AV-78, extensional epidote vein: sample WIS-014 766.83). Allanite and titanite in the Trill amphibole amygdule assemblage (sample TR-1005) show REE values as high as silicate minerals in the miarolitic cavities (sample 12AV-57) and pre-sulphide epidote veins.

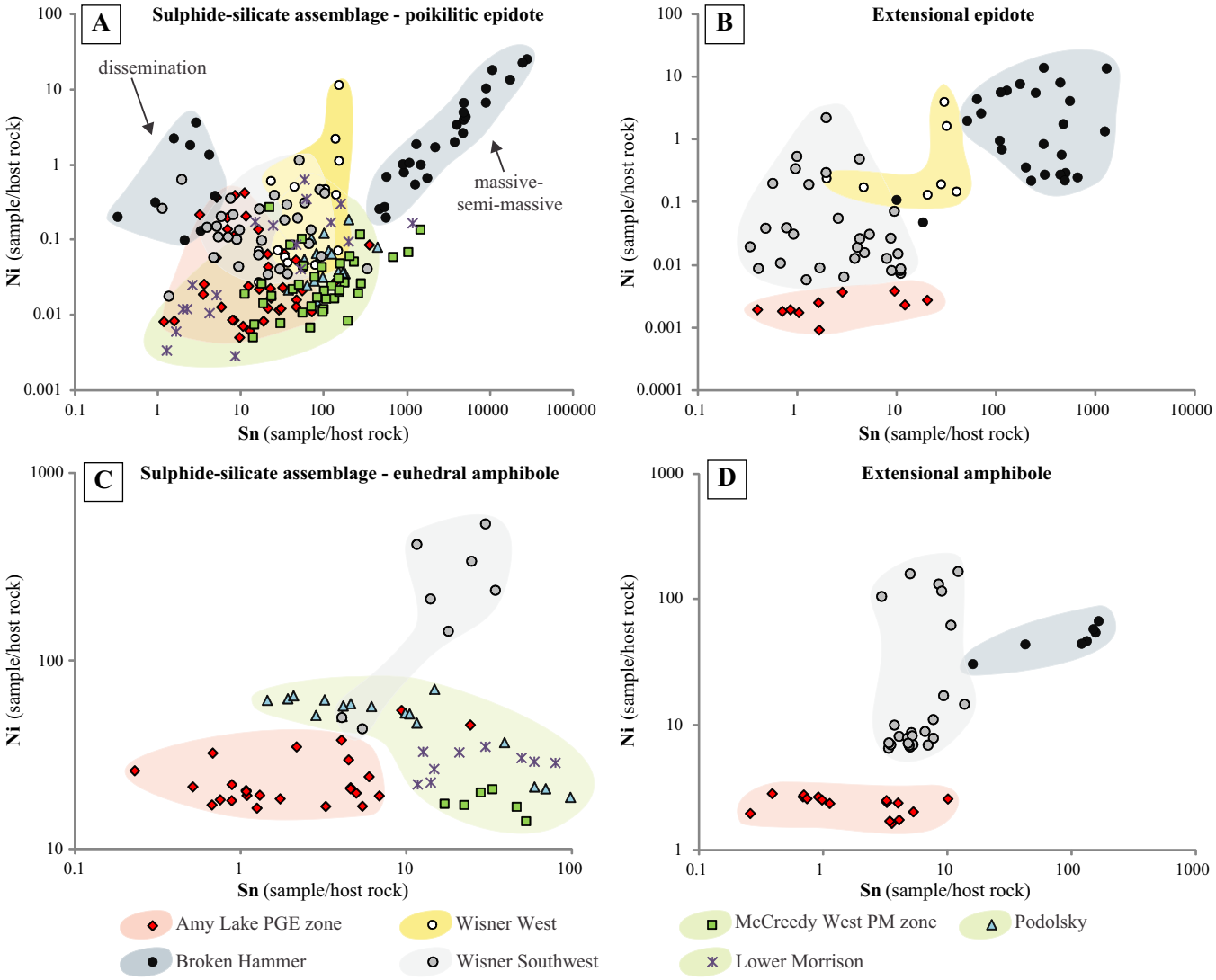

Figure 16. Sn and Ni in sulphide-associated and extensional epidote and amphibole samples (footwall mineralization, location-grouped). The relative position of the groups is similar in each diagram, indicating roughly constant Sn:Ni ratios associated with the different areas regardless to the analyzed mineral. The only difference is in the poikilitic epidote from disseminated sulphide samples from Broken Hammer, that form low-Sn group separated from massive-semi-massive samples from the same location.

the Broken Hammer sperrylite zone are unusually enriched (samples 12AV-16A, 12AV-17, and 12AV-15B; Appendix A, Figs. A2, A3).

In general, the relative concentrations of pathfinder elements in the silicate minerals are a good reflection of the relationship that was expected based on the mineral composition of alteration assemblages: the highest amounts of Ni, Co, Pb, and Sn were found in epidote and amphibole in footwall ore as well as in high-PGE pre-sulphide samples that contain Ni-sulphides and significant amounts of Pb- and Sn-bearing trace minerals. An important observation is that trace element fields of barren extensional epidote and amphibole veins completely overlap with the mineralized group (sulphide-silicate assemblage and Broken Hammer epidote-sperrylite assemblage) emphasizing a strong genetic relationship that was suggested by Tuba et al. (2014). High Ni-values in the minerals are also associated with high-PGE pre-sulphide samples, where minor to trace millerite may be present.

Although epidote and amphibole associated with footwall mineralization (both in the sulphide-silicate assemblage and extensional veins) occupy a wide field in the discrimination diagrams, systematic patterns are revealed when plotted according to geographic location. The relative enrichment of Ni, Sn, Co, and Zn is very similar between the mineralized areas, regardless of the mineral species and alteration group analyzed (Figs. 16, 17, and 18).

Broken Hammer silicates are enriched in Sn relative to the other mineralized environments, and they are also characterized by anomalously high Ni values (Fig. 16). At Broken Hammer, Sn and Ni values correlate well in poikilitic epidote from the selvage of sulphide

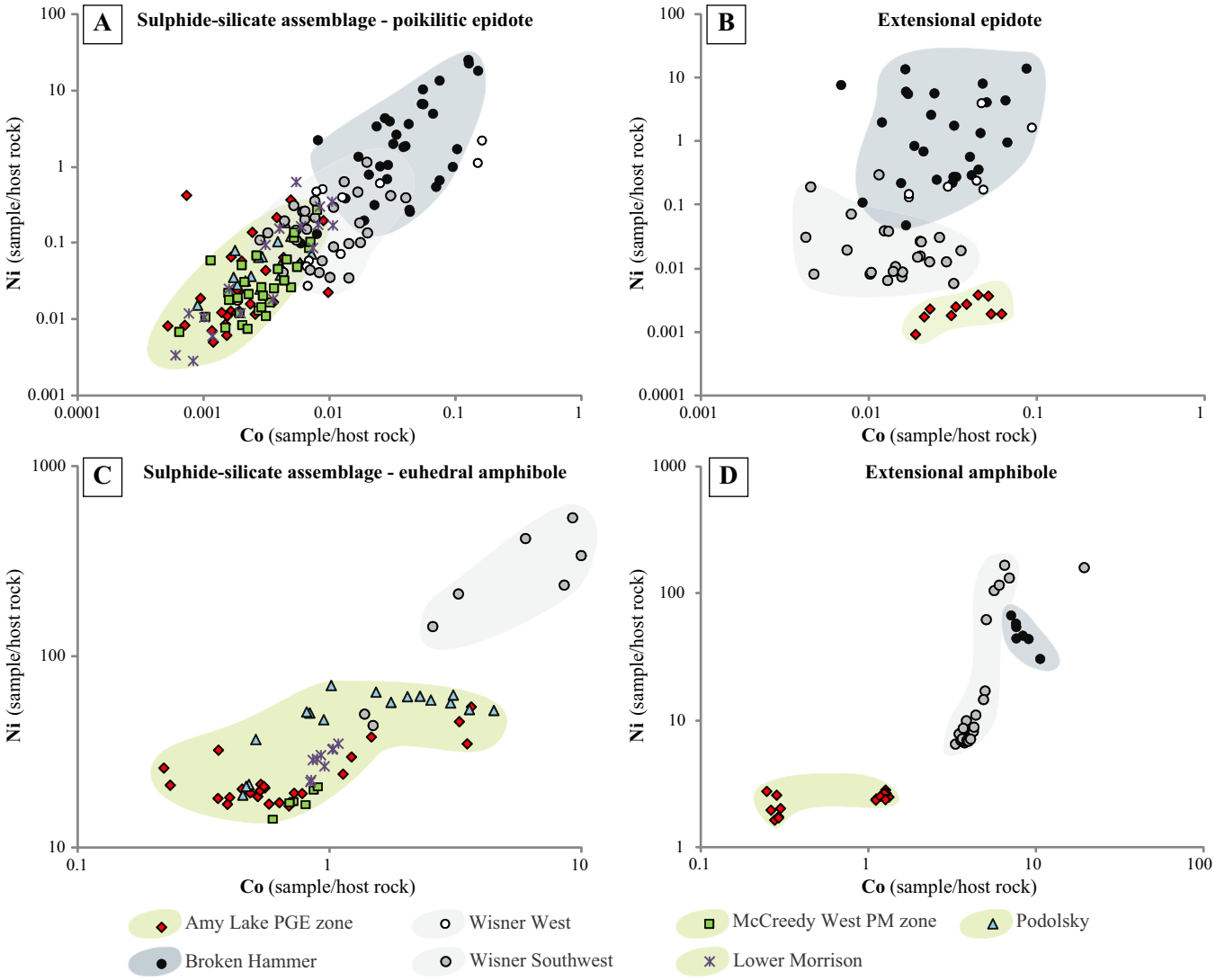

Figure 17. Co and Ni in sulphide-associated and extensional epidote and amphibole samples (footwall mineralization, grouped by geographical location). The relative position of the groups is similar in each diagram, indicating roughly constant Co:Ni ratios that are highest in the Wisner areas. The exception is Co in extensional epidote, where it shows the same ranges in all groups.

veins, with higher values represented by massive sulphide samples and lower Sn and Ni values in semi-massive sulphides. Poikilitic epidote found disseminated in the halo of an extensional amphibole vein has low Sn concentrations and does not show a correlation with Ni content. Poikilitic and extensional epidote from Wisner West have similarly high Ni values but lower Sn values than the Broken Hammer samples (amphibole was not analyzed from Wisner West.) At Amy Lake on the East Range, all silicates are dominantly low in both Sn and Ni content, with a few outliers among the poikilitic epidote. The Wisner Southwest zone differs from the Amy Lake area in that it generally has higher Ni values. Only poikilitic epidote and the associated euhedral amphibole were analyzed from Podolsky, Lower Morrison, and the PM zone orebodies; the analyses scatter in the middle range of Sn content and the lower to middle portion of the diagram concerning Ni content (Fig. 16).

Cobalt and Ni correlate well in poikilitic epidote at the database scale. The relative enrichment of Co versus Ni among the silicates from the different areas mimics the pattern of Sn versus Ni (Fig. 17). Where data are available (poikilitic epidote and extensional amphibole), Broken Hammer samples represent the most enriched group, followed by Wisner West and Southwest samples. The lowest relative Co and Ni concentrations again show up in the Amy Lake, Podolsky, Lower Morrison, and PM zone silicates, with the Podolsky deposit signature overlapping but containing the most Co- and Ni-enriched euhedral amphibole of the intermediate group (Fig. 17). Extensional epidote only partly shows this trend; Co concentration in the groups scatter over a similar range.

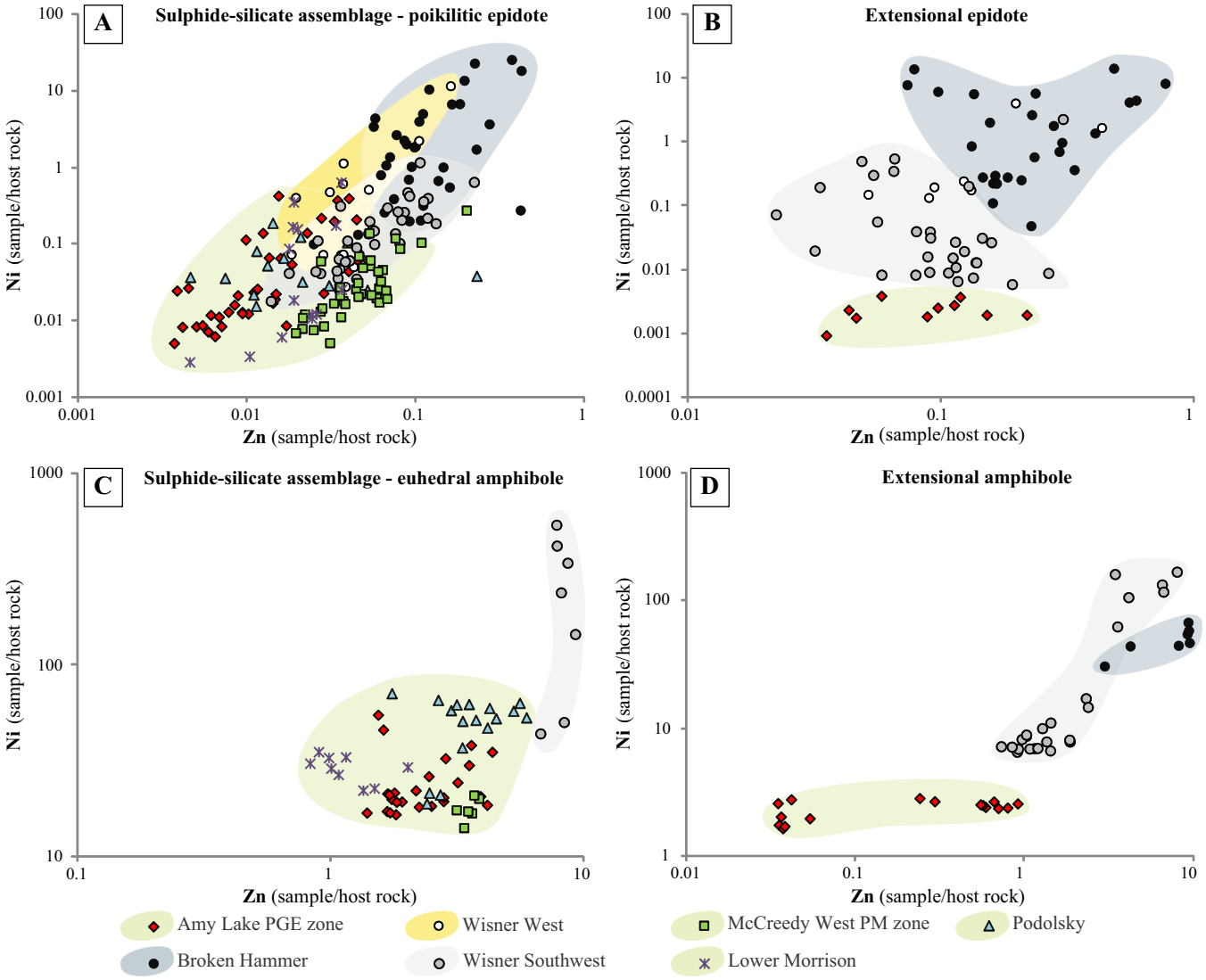

Figure 18. Zn and Ni in sulphide-associated and extensional epidote and amphibole samples (footwall mineralization, grouped by geographical location). The relative position of the groups is similar in each diagram, indicating roughly constant Zn:Ni ratios that are highest in the Wisner areas. The exception is Zn in extensional epidote, where it shows the same ranges in all groups.

The difference in Zn content is not very pronounced among the different areas, although the Wisner zones (Broken Hammer, Wisner West, and Southwest) tend to be more enriched than the others (Fig. 18). Extensional epidote also shows similar ranges in all available samples.

CONCLUSIONS AND SUMMARY

To properly classify and fingerprint alteration assemblages indicative of Sudbury footwall Cu-PGE mineralization, an extensive suite of 62 samples representing a diversity of post-impact alteration assemblages was analyzed by in situ LA-ICP-MS. Trace element data of 54 elements were collected from epidote, allanite, amphibole, and titanite to establish typical element associations and classification criteria, with special emphasis on alteration assemblages, to test the robustness of the PGE ore geochemical fingerprint.

Epidote and amphibole in the alteration assemblages exhibit host-rock normalized REE plots with characteristic topologies that are best described with nLREE to nHREE relations. Based on the REE data of all available minerals from a particular sample, high-REE (with additional Y, Th, and U) assemblages are found in miarolitic cavities and pervasive epidote-amphibole alteration that predate the Sudbury footwall mineralization. Vein-type pre-sulphide assemblages are comparably depleted in REE, whereas sulphide-silicate assemblages of footwall mineralization and associated extensional silicate veins, as well as post-Sudbury shear-type veins are REE-poor. The amount of REE, Y, Th, and U is interpreted to reflect the composition of the parental fluids.

Pathfinder elements Ni, Pb, Sn, and Co are most distinctive/indicative in fingerprinting the ore-bearing alteration assemblages. The highest concentrations are

associated with silicates from footwall mineralization and the accompanying extensional veins, emphasizing the genetic link between the two assemblages. High-PGE pre-sulphide assemblages are characterized by high Ni and Co but low Pb and Sn values. Other assemblages are notably depleted in these elements.

Epidote and amphibole of mineralized sulphide-silicate and generally barren extensional assemblages show differences in the concentrations of key pathfinders among different locations along the North and East ranges. The Wisner area, especially the Broken Hammer zone, is characterized by the highest Sn, Ni, Co, and Zn values, whereas silicates in the Amy Lake PGE zone are usually the poorest in these elements. Podolsky, Lower Morrison, and PM zone samples form a group in-between.

The trace element concentration of the alteration minerals was likely influenced by (1) the composition of the parental fluid (e.g. REE, U, Th, Ni, Pb, Sn), (2) the host rock, particularly mafic rocks (e.g. As, Zn) and/or (3) the crystal structural properties of the minerals (e.g. Mg and Sr in epidote).

Element partitioning occurs between texturally coeval minerals, such as epidote and amphibole (REE, Pb, Bi, Sn: affinity to epidote; Co, Ni, Zn: affinity to amphibole), as well as titanite and amphibole (REE, Sn, Zr, Nb, Yb, Th, U: affinity to titanite; Co, Ni, Zn: affinity to amphibole). This scavenging phenomenon greatly affects the element distribution of the mineral pairs; therefore, conclusions drawn on trace element concentrations of a single participant should be avoided. The necessity to analyze all major and minor mineral phases and to discuss them in context is emphasized here.

ACKNOWLEDGEMENTS

The authors would like to thank the exploration and mining companies Wallbridge Mining, FNX/KGHM, and Vale for access to properties, orebodies, and drill core. The GSC mineralogy group is thanked, particularly Pat Hunt and Katherine Venance, for their often last-minute analyses. Zhaoping Yang and Simon Jackson provided expert advice to the first author in the laser ablation ICP-MS lab.

REFERENCES

Abramov, P. and Kring, D.A., 2004. Numerical modelling of an impact-induced hydrothermal system at the Sudbury crater; Journal of Geophysical Research, v. 109, E10007, 16 p.

Ames, D.E., 1999. Geology and regional hydrothermal alteration of the crater-fill, Onaping Formation: Association with Zn-Pb-Cu mineralization, Sudbury structure, Canada; Ph.D. thesis, Carleton University, Ottawa, Ontario, 460 p.

Ames, D.E. and Farrow, C.E.G., 2007. Metallogeny of the Sudbury mining camp, Ontario, *In:* Mineral Deposits of Canada: A Synthesis of Major Deposit Types, District Metallogeny, the Evolution of Geological Provinces, and Exploration methods, (ed.) W.D. Goodfellow; Geological Association of Canada, Mineral Deposits Division, Special Publication 5, p. 329–350.

Ames, D.E. and Gibson, H.L., 1995. Controls on and geological setting of regional hydrothermal alteration within the Onaping Formation, footwall to the Errington and Vermilion base metal deposits, Sudbury Structure, Ontario; Geological Survey of Canada, Current Research 1995-E, p. 161–173.

Ames, D.E. and Gibson, H.L., 2004a. Geology, alteration and mineralization of the Onaping Formation, Rockcut Lake area, Norman Township, Sudbury, Ontario; Geological Survey of Canada, Open File 4565.

Ames, D.E. and Gibson, H.L. 2004b. Geology, alteration and mineralization of the Onaping Formation, Joe Lake area, Wisner Township, Sudbury, Ontario; Geological Survey of Canada Open File 4566.

Ames, D.E. and Houlé, M.G., 2011. Overview of the Targeted Geoscience Initiative 4 nickel-copper platinum group elements-chromium project (2010–2015)—mafic to ultramafic ore systems: footprint, fertility and vectors, *In:* Summary of Field Work and Other Activities 2011; Ontario Geological Survey, Open File Report 6270, p. 37-1 to 37-7.

Ames, D.E. and Houlé, M.G. (ed.), 2015. Targeted Geoscience Initiative 4: Canadian Nickel-Copper-Platinum Group Elements-Chromium Ore Systems — Fertility, Pathfinders, New and Revised Models; Geological Survey of Canada, Open File 7856.

Ames, D.E. and Kjarsgaard, I., 2013. Sulphide and alteration mineral chemistry of low- and high-sulphide Cu-PGE-Ni deposits in the footwall environment, Sudbury, Canada; Geological Survey of Canada, Open File 7331.

Ames, D.E., Watkinson, D.H., and Parrish, R.R., 1998. Dating of a regional hydrothermal system induced by the 1850 Ma Sudbury impact event; Geology, v. 26, p. 447–450.

Ames, D.E, Golightly, J.P., Lightfoot, P.C., and Gibson, H.L., 2002. Vitric compositions in the Onaping Formation and their relationship to the Sudbury Igneous Complex, Sudbury structure; Economic Geology, v. 97, p. 1541–1562.

Ames, D.E., Buckle, J., Davidson, A., and Card, K., 2005, Sudbury bedrock compilation: Geological Survey of Canada Open File 4570, geology, color map, and digital tables, scale 1:50,000.

Ames, D.E., Jonasson, I.R., Gibson, H.L., Pope, K.O., 2006. Impact-generated hydrothermal system- Constraints from the large Paleoproterozoic Sudbury crater, Canada, *In:* Biological Processes Associated with Impact Events, (ed.) C. Cockell, I. Gilmour, and C. Koeberl; Springer-Verlag Berlin-Heidelberg, Impact Studies, p. 55–100.

Ames, D.E., McClenaghan, M.B., and Averill, S., 2007. Footwall-hosted Cu-PGE (Au, Ag), Sudbury Canada: Towards a new exploration vector, *In:* Abstracts; Fifth Decentennial International Conference on Mineral Exploration, September 2007, Toronto, Canada.

Ames, D.E., Davidson, A., and Wodicka, N., 2008. Geology of the Giant Sudbury polymetallic mining camp, Ontario, Canada; Economic Geology, v. 103, p. 1057–1077.

Ames, D.E., Dare, S.A., Hanley, J.J., Hollings, P., Jackson, S., Jugo, P.J., Kontak, D., Linnen, R., and Samson, I.M., 2012. Update on research activities in the Targeted Geoscience Initiative 4 magmatic hydrothermal nickel-copper-platinum group elements ore system subproject: system fertility and ore vectors, *In:* Summary of Field Work and Other Activities 2012; Ontario Geological Survey, Open File Report 6280, p. 41-1 to 41-11.

Ames, D.E., Hanley, J., Tuba, G., and Jackson, S., 2013. High-grade sperrylite zone reveals primitive source in the Sudbury impact structure; Mineralogical Magazine, v. 77, p. 587.

Ames, D.E., Hanley, J.J., and Jackson, S.E., 2014. Low sulfide high-grade sperrylite-epidote-quartz zone, (Sudbury, Canada): implications for hydrothermal-magmatic processes, *In:* Abstracts; International Mineralogical Association, Johannesburg, South Africa.

Bleeker, W., Kamo, S., and Ames, D., 2013. New field observations and U-Pb age data for footwall (target) rocks at Sudbury: Towards a detailed cross-section through the Sudbury Structure, *In:* Extended Abstracts; Lunar and Planetary Institute Conference, Sudbury, Ontario.

Bleeker, W., Kamo, S.L., Ames, D.E., and Davis, D., 2015. New field observations and U-Pb ages in the Sudbury area: toward a detailed cross-section through the deformed Sudbury Structure, *In:* Targeted Geoscience Initiative 4: Canadian Nickel-Copper-Platinum Group Elements-Chromium Ore Systems — Fertility, Pathfinders, New and Revised Models, (ed.) D.E. Ames and M.G. Houlé; Geological Survey of Canada, Open File 7856, p. 151–166.

Campos-Alvarez, N., Samson, I.M., Fryer, B.J., and. Ames, D.E., 2010. Sr isotopic composition of hydrothermal epidote and carbonate in the Sudbury structure from LA-ICPMS analysis: Implications for fluid sources and architecture; Chemical Geology, v. 278, p. 131–150.

Carter, W.M., Watkinson, D.H., Ames, D.E., and Jones, P.C., 2009. Emplacement of quartz dioritic magmas and Cu-(Ni)-PGE mineralization of the Whistle Offset, Sudbury Canada; Geological Survey of Canada, Open File 6134, 54 p.

Farrow, C.E.G., 1994. Geology, alteration, and the role of fluids in Cu-Ni-PGE mineralization of the footwall rocks to the Sudbury Igneous Complex, Levack and Morgan Townships, Sudbury District, Ontario; Ph.D. thesis, Carleton University, Ottawa, Canada, 373 p.

Farrow, C.E.G. and Watkinson, D.H., 1992. Alteration and the role of fluids I Ni, Cu and platinum-group element deposition, Sudbury igneous complex contact, Onaping-Levack Area, Ontario; Mineralogy and Petrology, v. 46, p. 67–83.

Farrow, C.E.G. and Watkinson, D.H., 1996. Geochemical evolution of the Epidote Zone, Fraser mine, Sudbury, Ontario: Ni-Cu-PGE remobilization by saline fluids; Exploration and Mining Geology, v. 5, p. 17–31.

Farrow, C.E.G. and Watkinson, D.H., 1999. An evaluation of the role of fluids in Cu-Ni-PGE-bearing mafic-ultramafic systems; Geological Association of Canada, Short Course notes, v. 13, p. 31–67.

Farrow, C.E.G. and Lightfoot, P.C., 2002. Sudbury PGE revisited: Towards an integrated model, *In:* The Geology, Geochemistry, Mineralogy and Mineral Beneficiation of Platinum-Group Elements, (ed.) L.J. Cabri; Canadian Institute of Mining, Metallurgy and Petroleum, p. 273–297.

Farrow, C.E.G., Everest, J.O., King, D.M., and Jolette, C., 2005. Sudbury Cu-(Ni)-PGE systems: Refining the classification using McCreedy West mine and Podolsky project case studies, *In:* Exploration for Deposits of Platinum-Group Elements, (ed.) J.E. Mungall; Mineralogical Association of Canada, Short Course Series v. 35, p. 163–180.

Frei, D., Liebscher, A., Franz, G., and Dulski, P., 2004. Trace element geochemistry of epidote minerals; Reviews in Mineralogy and Geochemistry, v. 56, p. 553–605.

Hanley, J.J. and Mungall, J.E., 2003. Chlorine enrichment and hydrous alteration of the Sudbury Breccia hosting footwall Cu-Ni-PGE mineralization at the Fraser mine, Sudbury, Ontario, Canada; The Canadian Mineralogist, v. 41, p. 857–881.

Hanley, J.J. and Bray, C.J., 2009. The trace metal content of amphibole as a proximity indicator for Cu-Ni-PGE mineralization in the footwall of the Sudbury Igneous Complex, Ontario, Canada; Economic Geology, v. 104, p. 113–125.

Hanley, J.J., Mungall, J.E., Bray, C.J., and Gorton, M.P., 2004. The origin of bulk and water-soluble Cl and Br enrichments in ore-hosting Sudbury Breccia in the Fraser Copper Zone, Strathcona Embayment, Sudbury, Ontario, Canada; The Canadian Mineralogist, v. 42, p. 1777–1798.

Hanley, J.J., Mungall, J.E., Pettke, T., Spooner, E.T.C., and Bray, C.J., 2005. Ore metal redistribution by hydrocarbon-brine and hydrocarbon-halide melt phases, North Range footwall of the Sudbury Igneous Complex, Ontario, Canada; Mineralium Deposita, v. 40, p. 237–256.

Hanley, J., Ames, D., Barnes, J., Sharp, Z., and Guillong, M., 2011. Interaction of magmatic fluids and silicate melt residues with saline groundwater in the footwall of the Sudbury Igneous Complex, Ontario, Canada: New evidence from bulk rock geochemistry, fluid inclusions and stable isotopes; Chemical Geology, v. 281, p. 1–25.

Kerr, M., Hanley, J., Morrison, G., Everest, J., and Bray, C., 2015. Preliminary evaluation of trace hydrocarbon speciation and abundance as exploration tool for footwall-style sulfide ores associated with the Sudbury Igneous Complex, Ontario, Canada; Economic Geology, v. 110, p. 50–76.

Kjarsgaard, I.M. and Ames, D.E., 2010. Ore mineralogy of Cu-Ni-PGE deposits in the North Range footwall environment, Sudbury, *In:* Abstracts, (ed.) P.J. Jugo, C.M. Lesher, and J.E. Mungall; 11th International Platinum Symposium, 2010, Sudbury, Ontario, Canada, Ontario Geological Survey, Miscellaneous Release Data 269.

Krogh, T.E., Davis, D.W., and Corfu, F., 1984. Precise U-Pb zircon and baddelyite ages for the Sudbury area, *In:* The Geology and Ore Deposits of the Sudbury Structure, (ed.) E.G. Pye, A.J. Naldrett and P.E. Giblin; Ontario Geological Survey, Special Volume 1, p. 431–446.

Li, C. and Naldrett, A.J., 1994. A numerical model for the compositional variations of Sudbury sulfide ores and its application of exploration; Economic Geology, v. 89, p. 1599–1607.

Jago, B.C., Morrison, G.G., and Little, T.L., 1994. Metal zonation patterns and microtextural and micromineralogical evidence for alkali- and halogen-rich fluids in the genesis of the Victor Deep and McCreedy East footwall copper orebodies, Sudbury Igneous Complex, *In:* Proceedings of the Sudbury-Noril'sk Symposium; Ontario Geological Survey, Special Publication 5, p. 65–75.

Lightfoot, P.C., Keays, R.R., Morrison, G.C., Bite, A., and Farrell, K.P., 1997. Geologic and geochemical relationships between the Contact Sublayer, inclusions, and the Main Mass of the Sudbury Igneous Complex: A case study of the Whistle Mine Embayment; Economic Geology, v. 92, p. 647–673.

MacInnis, L.M., Kontak, D.J., Ames, D.E., and Joyce, N.L., 2014. Geochemistry and supporting databases from an alteration study at the Podolsky Cu(-Ni)-PGE deposit, Whistle offset structure, Sudbury; Geological Survey of Canada, Open File 7666; 19 p. doi:10.4095/295482

Magyarosi, Z., Watkinson, D.H., and Jones, P.C., 2002. Mineralogy of Ni-Cu-platinum-group element sulfide ore in the 800 and 810 orebodies, Copper Cliff South mine, and P-T-X conditions during the formation of platinum-group minerals; Economic Geology, v. 97, p. 1471–1486.

Melosh, H. J., 1989, Impact Cratering: A Geological Process; Oxford University Press, New York, 25 p.

Molnár, F., Watkinson, D.H., and Jones, P.C., 2001, Multiple hydrothermal processes in footwall units of the North Range, Sudbury Igneous Complex, Canada, and implications for the genesis of vein-type Cu-Ni-PGE deposits; Economic Geology, v. 96, p. 1645–1670.

Nelles, E.W., Lesher, C.M., and Lafrance, B., 2010, Mineralogy and textures of Cu-PPGE-Au-rich mineralization in the

Morrison (Levack footwall) Deposit, Sudbury, Ontario, *In:* Abstracts; Society of Economic Geologists, 2010 Conference, October 2010, Keystone, USA

Péntek, A., 2009. Partial melting and melt segregation within the contact aureole of the Sudbury Igneous Complex (Ontario, Canada) and their significance in hydrothermal Cu-Ni-PGE mineralization of the footwall; Ph.D. thesis, Eötvös Loránd University, Budapest, Hungary, 163 p.

Péntek, A., Molnár, F., Watkinson, D.H., and Jones, P.C., 2008. Footwall-type Cu-Ni-PGE mineralization in the Broken Hammer area, Wisner Township, North Range, Sudbury structure; Economic Geology, v. 103, p. 1005–1028.

Péntek, A., Molnár, F., Watkinson, D.H., Jones, P.C., and Mogessie, A., 2011. Partial melting and melt segregation in footwall units within the contact aureole of the Sudbury Igneous Complex (North and East ranges, Sudbury structure), with implications for their relationship to footwall Cu-Ni-PGE mineralization; International Geology Review, v. 53, p. 291–325.

Péntek, A., Molnár, F., Tuba, Gy., Watkinson, D.H., and Jones, P.C., 2013. The significance of partial melting processes in hydrothermal 'low-sulfide' Cu-Ni-PGE mineralization within the footwall of the Sudbury Igneous Complex, Ontario, Canada; Economic Geology, v. 108, p. 59–78.

Petrus, J.A., Ames, D.E., and Kambor, B.S., 2014. On the track of the elusive Sudbury impact: geochemical evidence for a chondrite or comet bolide; Terra Nova, v. 26, p. 1–12. doi:10.1111/ter.12125

Pope, K.O., Kieffer, S.W., and Ames, D.E., 2004. Empirical and theoretical comparisons of the Chicxulub and Sudbury impact craters; Meteoritics and Planetary Science, v. 39, p. 97–116.

Tuba, G., 2012. Multiple hydrothermal systems in the footwall of the Sudbury Igneous Complex: Fluid characteristics, associated alteration, and the role in footwall-type, low-sulphide" Cu-(Ni-)PGE sulphide mineralization (North and East Ranges, Sudbury structure, Canada); Ph.D. thesis, Eötvös Loránd University, Budapest, Hungary.

Tuba, G., Molnár, F., Watkinson, D.H., Jones, P.C., and Mogessie, A., 2010. Hydrothermal vein and alteration assemblages associated with low-sulfide footwall Cu-Ni-PGE mineralization and regional hydrothermal processes, North and East Ranges, Sudbury structure, Canada, *In:* The Challenge of Finding New Mineral Resources: Global Metallogeny, Innovative Exploration, and New Discoveries, (ed.) R.J. Goldfarb, E.E. Marsh, and T. Monecke; Society of Economic Geologists, Special Publication 15, v. 2, p. 573–598.

Tuba, G., Molnár, F., Ames, D.E., Péntek, A., Watkinson, D.H., and Jones, P.C., 2014. Multi-stage hydrothermal processes involved in "low-sulfide" Cu(-Ni)-PGE mineralization in the footwall of the Sudbury Igneous Complex (Canada): Amy Lake PGE zone, East Range; Mineralium Deposita 49, p. 7–47.

White, C.J., 2010. Low-sulfide PGE-Cu-Ni mineralization from five prospects within the footwall of the Sudbury Igneous Complex, Ontario, Canada; Ph.D. thesis, University of Toronto, Toronto, Ontario, 337 p.

Wilson, B.S., 2012. New sperrylites from Canada; Minerals, the Collectors Newspaper, v. 4, p. 7–10.